THE JOURNAL OF BIOLOGICAL CHEMISTRY VOL. 292, NO. 8, pp. 3466–3480, February 24, 2017

Neuron-enriched RNA-binding Proteins Regulate Pancreatic Beta Cell Function and Survival*

Received for publication, July 14, 2016, and in revised form, January 10, 2017 Published, JBC Papers in Press, January 11, 2017, DOI 10.1074/jbc.M116.748335

Jonàs Juan-Mateu[‡1,2], Tatiana H. Rech[‡1,3], Olatz Villate[‡], Esther Lizarraga-Mollinedo[‡], Anna Wendt[§], Jean-Valery Turatsinze[‡], Letícia A. Brondani[‡], Tarlliza R. Nardelli[‡], Tatiane C. Nogueira[‡], Jonathan L. S. Esguerra[§], Maria Inês Alvelos[‡], Piero Marchetti[¶], Lena Eliasson[§], and Décio L. Eizirik[‡‖4]

From the [‡]ULB Center for Diabetes Research, Université Libre de Bruxelles, 1070 Brussels, Belgium, the [§]Lund University Diabetes Center, Unit of Islets Cell Exocytosis, Department of Clinical Sciences Malmö, Lund University, SE 205 02 Malmö, Sweden, the [¶]Department of Clinical and Experimental Medicine, Islet Cell Laboratory, University of Pisa, 56126 Pisa, Italy, and [‖]Welbio, Université Libre de Bruxelles, 808 Route de Lennik, CP618, 1070 Brussels, Belgium

Edited by Jeffrey E. Pessin

Pancreatic beta cell failure is the central event leading to diabetes. Beta cells share many phenotypic traits with neurons, and proper beta cell function relies on the activation of several neuron-like transcription programs. Regulation of gene expression by alternative splicing plays a pivotal role in brain, where it affects neuronal development, function, and disease. The role of alternative splicing in beta cells remains unclear, but recent data indicate that splicing alterations modulated by both inflammation and susceptibility genes for diabetes contribute to beta cell dysfunction and death. Here we used RNA sequencing to compare the expression of splicing-regulatory RNA-binding proteins in human islets, brain, and other human tissues, and we identified a cluster of splicing regulators that are expressed in both beta cells and brain. Four of them, namely Elavl4, Nova2, Rbox1, and Rbfox2, were selected for subsequent functional studies in insulin-producing rat INS-1E, human EndoC-βH1 cells, and in primary rat beta cells. Silencing of Elavl4 and Nova2 increased beta cell apoptosis, whereas silencing of Rbfox1 and Rbfox2 increased insulin content and secretion. Interestingly, Rbfox1 silencing modulates the splicing of the actin-remodeling protein gelsolin, increasing gelsolin expression and leading to faster glucose-induced actin depolymerization and increased insulin release. Taken together, these findings indicate that beta cells share common splicing regulators and programs with neurons. These splicing regulators play key roles in insulin release and beta cell survival, and their dysfunction may contribute to the loss of functional beta cell mass in diabetes.

Insulin-secreting pancreatic beta cells share many phenotypic traits with neurons. Similarities range from an analogous physiology and function to similar development and gene expression (1). Beta cells release insulin using a similar exocytotic machinery as used by neurons to release neurotransmitters. Indeed, insulin is stored and secreted using scaffolding proteins and synaptic-like vesicles similar to neuronal cells (2–4), and like neurons, beta cells are able to generate action potentials in response to different stimuli (5). Despite having different embryonic origins (6, 7), global gene expression and active chromatin marks of beta cells are closer to neural tissues than to any other tissue, including other pancreatic cells (8). Neurons are phylogenetically older than beta cells, and in some primitive organisms neurons express insulin and regulate circulating glucose levels (9, 10). Taken together, these findings suggest that beta cells have evolved into specialized insulin-secretory cells by adopting, at least in part, neuronal transcription programs (1). Supporting this hypothesis, both neurons and beta cells lose the expression of the transcriptional repressor element-1 silencing transcription factor (REST)[5] during differentiation (11). REST is expressed in most non-neuronal cells and acts as a master negative regulator of neurogenesis by repressing a subset of neuron-specific genes that play a pivotal role in the development of the neuronal phenotype (12). In beta cells, the absence of REST allows the expressions of transcription factors and genes of the exocytotic machinery that are crucial for beta cell differentiation, survival, and secretory function (11–15).

Understanding how beta cells acquire neuron-like features has focused mainly on transcription, but it remains unclear whether beta cells and neurons share similar post-transcriptional

* This work was supported in part by European Union Project T2DSystems in the Horizon 2020 Programme of the European Commission; Fonds National de la Recherche Scientifique (FNRS) Grants T.0036.13 and FRFS-Welbio CR-2015A-06, Belgium; the Swedish Research Council project grants (to L. E.); the Juvenile Diabetes Foundation; the Helmsley Type 1 Diabetes Program; and National Institutes of Health NIDDK-HIRN Consortium 1UC4DK104166-01. The authors declare that they have no conflicts of interest with the contents of this article. The content is solely the responsibility of the authors and does not necessarily represent the official views of the National Institutes of Health.

[1] Both authors contributed equally to this work.

[2] Supported by MSCA Fellowship Grant from the Horizons 2020 European Union Program Project Reference 660449. To whom correspondence and reprint requests may be addressed: ULB Center for Diabetes Research, Université Libre de Bruxelles, Route de Lennik 808, 1070 Brussels, Belgium. Tel.: 32-2-555-63-05; Fax: 32-2-555-62-39; E-mail: mjuanmat@ulb.ac.be.

[3] Supported by Post-doctoral Fellowship Process Number CSF 12108-13-8 from CAPES, Brazil.

[4] To whom correspondence and reprint requests may be addressed: ULB Center for Diabetes Research, Université Libre de Bruxelles, Route de Lennik 808, 1070 Brussels, Belgium. Tel.: 32-2-555-63-05; Fax: 32-2-555-62-39; E-mail: deizirik@ulb.ac.be.

[5] The abbreviations used are: REST, repressor element-1 silencing transcription factor; AS, alternative splicing; RBP, RNA-binding protein; KD, knockdown; FACS, fluorescence-activated cell sorting; m.o.i., multiplicity of infection; qRT, quantitative RT; FCCP, carbonyl cyanide *p*-trifluoromethoxyphenylhydrazone.

regulation. Alternative splicing (AS) is a key post-transcriptional mechanism that allows cells to fine-tune their transcriptome and generate proteome diversity to gain functional specialization. By regulating splice site selection and inclusion of alternative exons into mature mRNAs, AS enables individual genes to produce multiple protein isoforms that often display different properties or functions (16). AS is particularly widespread in the brain, playing a central role in neuronal development, complexity, and physiology (17, 18). Indeed, defects in splicing regulation are associated with a wide spectrum of neuropsychiatric and neurological disorders (19, 20). Neuron splicing programs are controlled by specific RNA-binding proteins (RBPs) that regulate the splicing of genes involved in key neuronal functions such differentiation, morphology, migration, electrophysiological activity, and synapse formation (21–23).

Beta cell failure is the central event leading to diabetes. Although the role of AS in the development of diabetes remains to be clarified, recent studies from our group indicate that AS alterations induced by both inflammation and disease susceptibility genes contribute to beta cell dysfunction and death (24–26). Furthermore, we found that the "neuron-specific" splicing factor Nova1 is expressed in beta cells (24) and regulates AS of genes involved in exocytosis and apoptosis (27).

In this study, we examined the expression of splicing-regulatory RBPs in pancreatic islets, brain, and other human tissues and detected a group of splicing regulators that are preferentially expressed in human islets and brain. We next focused on four of them, namely Elavl4 (also known as HuD), Nova2, Rbfox1, and Rbfox2. We confirmed their expression in pancreatic beta cells and identified their roles in beta cell function and survival. The findings obtained suggest that beta cells and neurons share common splicing programs and indicate that defects in splicing regulation of common brain-beta cells RBPs may contribute to beta cell dysfunction and death.

Results

Pancreatic Beta Cells Express Neuron-enriched RNA-binding Proteins—We used a previous RNA sequencing dataset of human islets (24) and the Illumina BodyMap 2.0 (GEO: GSE30611) to compare the expression of 118 splicing-regulatory RBPs between human islets and 16 other tissues. Some brain-expressed RBPs clustered together with the five human islet preparations evaluated, and we identified a group of RBPs that are relatively highly expressed in both human islets and brain (Fig. 1*A, yellow square*). This includes members of the ELAVL, RBFOX, and NOVA families of splicing-regulatory RBPs that have been reported previously to regulate key splicing programs in brain (18, 19). The expression of ELAVL4, NOVA2, RBFOX1, and RBFOX2 was confirmed in human islets and in the human insulin-producing EndoC-βH1 cell line by real time qPCR (Fig. 1, *B–E*). Of note, NOVA2, RBFOX1, and RBFOX2, but not ELAVL4, were also well expressed in adipose tissue. To understand the reasons for the similar RBPs gene expression pattern observed between human islets and brain, we assessed whether their expression was under the control of the transcriptional repressor REST. Gene expression of RBPs in rat INS-1E cells was analyzed after infection with an adenovirus encoding *REST* (Fig. 2*A*). REST overexpression down-regulated the expression of Snap25 (Fig. 2*B*), a known target of REST, but it did not modify the expression of Elavl4, Nova2, or Rbfox2, suggesting that these genes are not targets of REST in beta cells (Fig. 2, *C*, *D*, and *F*). REST overexpression down-regulated the expression of Rbfox1 (Fig. 2*E*), but the finding that Rbfox1 is expressed in other non-neuronal tissues (Fig. 1*D*) argues against a direct transcriptional regulation by REST. Compensatory cross-regulation between RBP paralogs was observed for Elavl4 and Nova2. Elavl4 knockdown (KD) by small interfering RNA (siRNA) increased the levels of paralog Elavl1 (Fig. 3, *A* and *B*). Similar observations were made for Nova1 expression under Nova2 KD (Fig. 3, *C* and *D*). However, no compensatory cross-regulation between Rbfox1 and Rbfox2 was observed (Fig. 3, *E–H*).

Elavl4 Modulates Beta Cell Death—To elucidate the function of Elavl4 in pancreatic beta cells, we used siRNAs to knock down Elavl4 in INS-1E, FACS-purified primary rat beta cells, and EndoC-βH1 cells (Fig. 4, *B*, *F,* and *H*). Elavl4 KD increased apoptosis under basal conditions but protected against cytokine-induced apoptosis in the three different cell models studied (Fig. 4, *C*, *G,* and *I*). Elavl4 KD affected neither glucose-stimulated insulin secretion nor insulin content (data not shown). Modulation of beta cell death following Elavl4 KD was secondary to activation of the mitochondrial pathway of apoptosis, as indicated by changes in the expression of cleaved caspase-3 and -9 measured by Western blotting (Fig. 4, *A*, *D,* and *E*). To identify the mechanisms underlying Elavl4 KD-induced apoptosis, we assessed the expression of several apoptotic regulators of the Bcl-2 family, as well as markers of endoplasmic reticulum stress and oxidative stress, but no changes were detected (data not shown).

Nova2 KD Increases Basal and Cytokine-induced Cell Death via the Mitochondrial Pathway of Apoptosis—Nova2 was silenced in INS-1E, EndoC-βH1, and FACS-purified primary rat beta cells (Fig. 5, *A*, *F,* and *H*). Nova2 KD increased INS-1E cell apoptosis under basal conditions and sensitized these cells to cytokine-induced apoptosis (Fig. 5*B*). This was accompanied by cleavage of caspase-9 and -3, indicating that cell death is secondary to the activation of the mitochondrial pathway of apoptosis (Fig. 5, *C–E*). Nova2 KD also increased apoptosis in FACS-purified primary rat beta cells and EndoC-βH1 cells (Fig. 5, *G* and *I*). Nova2 KD neither affected glucose-stimulated insulin release nor insulin content in INS-1E cells (data not shown).

Silencing of Rbfox1 and Rbfox2 Increases Insulin Secretion and Content—Rbfox1 and Rbfox2 were independently silenced in INS1-E cells (Figs. 6, *A* and *B,* and 7*A*). Rbfox1 silencing did not affect basal or cytokine-induced apoptosis (data not shown) but induced a significant increase in insulin release after glucose or glucose plus forskolin stimulation (Fig. 6, *C* and *D*). Interestingly, there was a dose-response relation between the induced Rbfox1 knockdown by the different siRNAs and the observed increase in insulin secretion. A similar phenotype was observed following Rbfox2 KD (Fig. 7*B*). In addition, increased K_{ATP}-channel independent insulin release was observed in Rbfox1 KD cells following stimulation with KCl (Fig. 6*E*). Moreover, insulin cellular content was significantly increased following Rbfox1 and Rbfox2 silencing (Figs. 6*F* and 7*C*). Insulin mRNA expression was significantly increased following Rbfox1

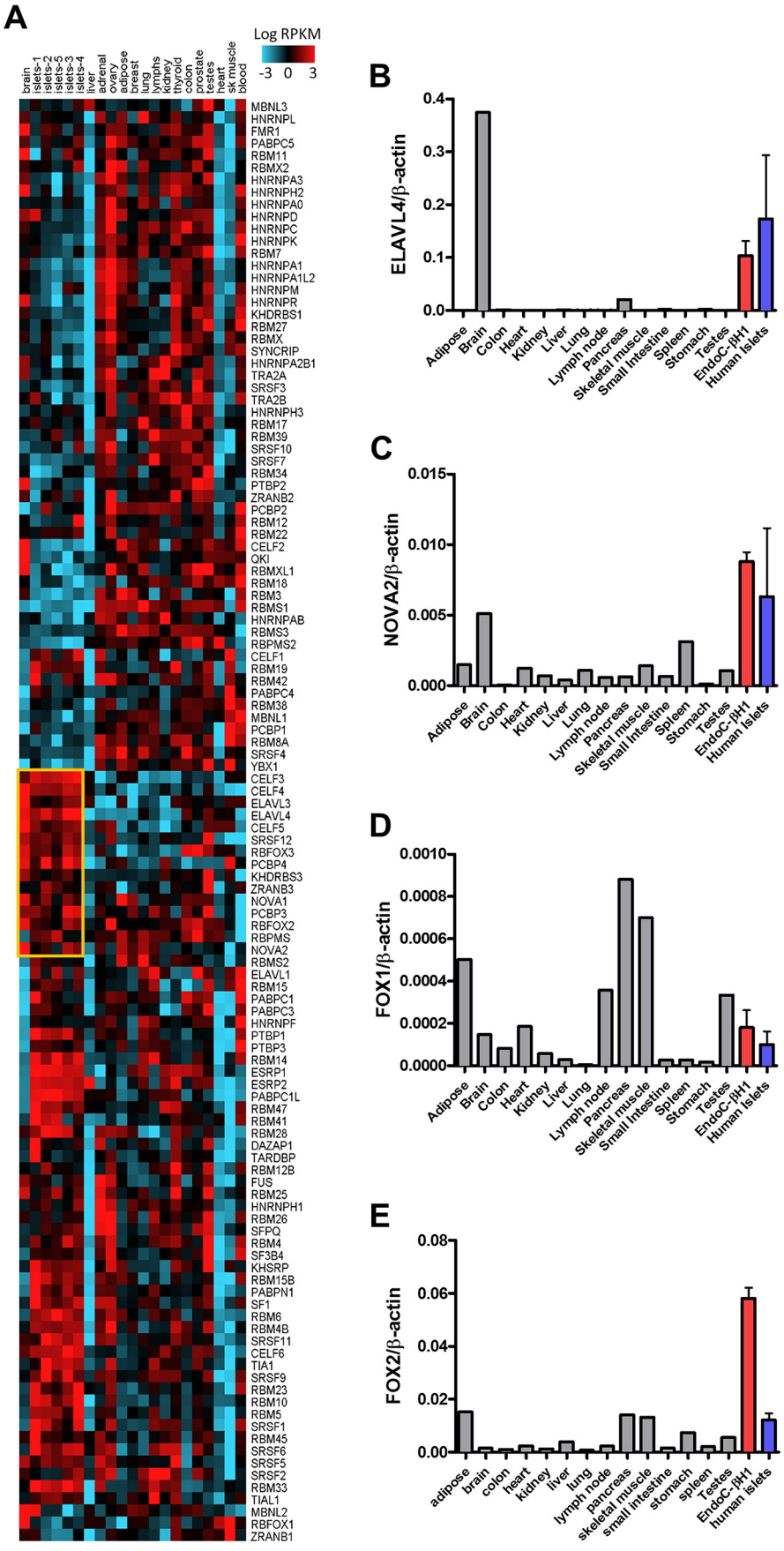

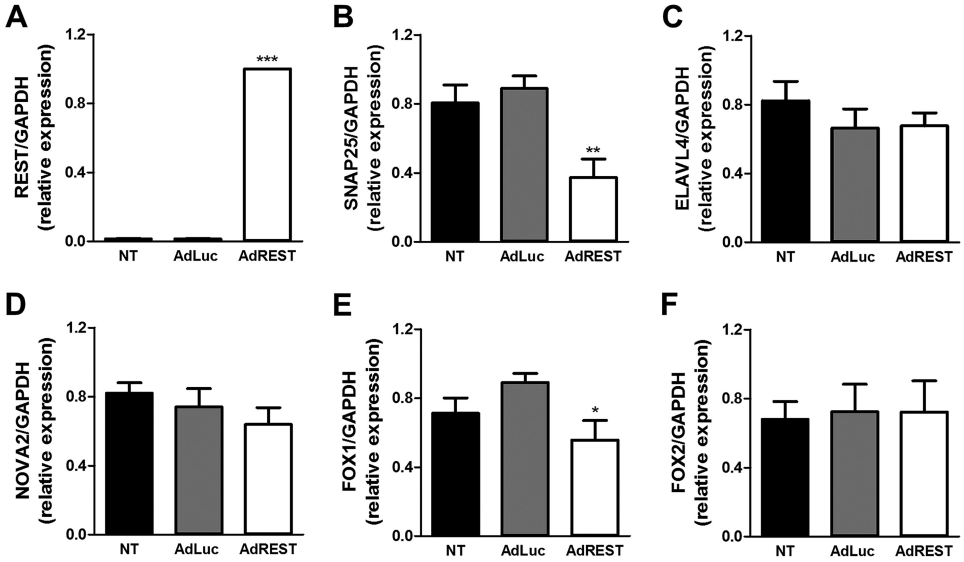

FIGURE 2. **Expression of neuron-enriched RBPs after REST overexpression in INS-1E cells.** INS-1E cells were infected with adenovirus overexpressing *Renilla* luciferase (*AdLuc*) or REST (*AdREST*) for 24 h at m.o.i. of 10 or left untreated (*NT,* non-treated). Expression of the following was measured by qRT-PCR and normalized by the housekeeping gene *Gapdh*: *A,* REST; *B,* Snap25; *C,* Elavl4; *D,* Nova2; *E,* Rbfox1; and *F,* Rbfox2. Results are mean ± S.E. of four to six independent experiments. *, $p < 0.05$; **, $p < 0.01$; and ***, $p < 0.001$ *versus* AdLuc; paired *t* test.

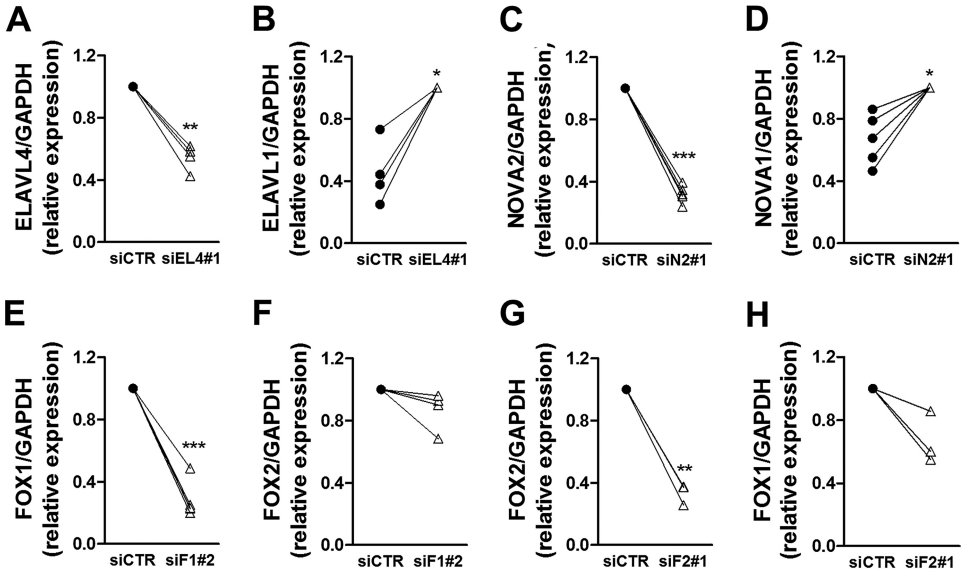

FIGURE 3. **Compensatory regulation within RBPs families.** INS-1E cells were transfected with siCTR or siRNAs targeting different RBPs for 48 h. The expression of the different RBPs was measured by qRT-PCR and normalized by the housekeeping gene *Gapdh*. Expression of the following was evaluated after Nova2 KD: *A,* Elavl4; *B,* Elavl1. Expression of Nova2 (*C*) and Nova1 (*D*) is shown. Expression of Rbfox1 (*E*) and Rbfox2 (*F*) was evaluated after Rbfox1 KD. Expression of Rbfox2 (*G*) and Rbfox1 (*H*) was evaluated after Rbfox2 KD. mRNA expression values were normalized by the highest value of each experiment, considered as 1. Results are from 3 to 5 independent experiments. *, $p < 0.05$; **, $p < 0.01$ and ***, $p < 0.001$ *versus* siCTR; paired *t* test.

KD by siFOX1#2 (the siRNA inducing more marked Rbfox1 inhibition) but not following KD with the less effective siFOX1#1 (Fig. 6*G*). To determine whether the observed increase in insulin secretion was secondary to increased glucose metabolism and ATP generation or due to augmented exocytosis, we measured glucose oxidation and mitochondrial function, and we analyzed calcium currents through patch clamp. No differences in glucose oxidation were observed between control and Rbfox1 KD cells (Fig. 6*H*). In line with this, there were no differences in mitochondrial function parameters such as glucose-induced respiration, ATP-linked respiration (response to oligomycin), and maximal respiration (response to FCCP following oligomycin), as evaluated by oxygen consumption rate measurements (Fig. 6*I*). Calcium currents were evoked by

FIGURE 1. **Pancreatic beta cells express neuron-enriched RNA-binding proteins.** *A,* heat map representing the expression of RBPs in human islets and in 16 other human tissues. Gene expression was assessed by RNA-sequencing using a previously published dataset consisting of five different human islets preparations (24) and the Illumina BodyMap 2.0. Expression values were hierarchically clustered using Gene Pattern modules. *Blue* and *red* colors indicate low and high expressed genes, respectively. RBPs showing high expression in brain and in human islets are highlighted by a *yellow square*. *B–E,* mRNA expression of four RBPs assessed by qRT-PCR in human islets ($n = 3$), insulin-producing EndoC-βH1 cells ($n = 3$), and in a panel of normal human tissues ($n = 1$). *B, ELAVL4*; *C, NOVA2*; *D, RBFOX1*; and *E, RBFOX2*.

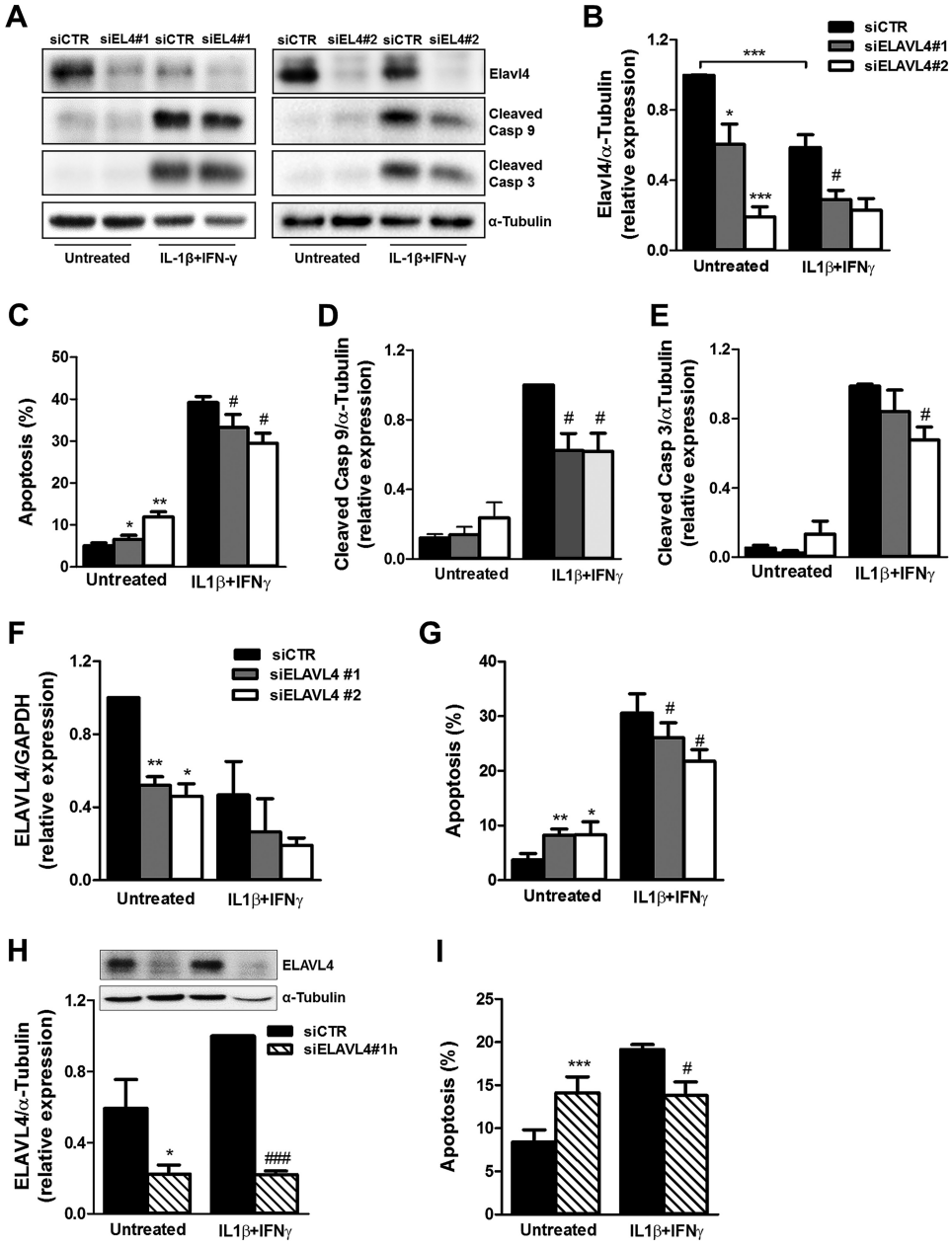

FIGURE 4. **Elavl4 modulates pancreatic beta cells death.** INS-1E cells (*A–E*), FACS-purified primary rat beta cells (*F* and *G*), and EndoC-βH1 cells (*H* and *I*) were transfected with siCTR or independent siRNAs targeting Elavl4 for 48 h and then exposed to the pro-inflammatory cytokines IL-1β + IFN-γ. Cytokine exposure was 24 h for INS-1E cells and 48 h for primary rat beta cells and EndoC-βH1 cells. *A,* two representative Western blottings showing Elavl4, cleaved caspase-9 and -3, and α-tubulin (used as loading control) after Elavl4 knockdown in INS-1E cells. *B,* Western blotting densitometric measurements of Elavl4. *C,* apoptosis in INS-1E cells was evaluated by propidium iodide staining. *D,* Western blotting densitometric measurements of cleaved caspase-9; *E,* cleaved caspase-3. *F,* mRNA expression of Elavl4 in FACS-purified primary rat beta cells measured by qRT-PCR and normalized by the housekeeping gene *Gapdh*; *G,* apoptosis evaluated by propidium iodide staining. *H,* protein expression of ELAVL4 and α-tubulin (used as loading control) in EndoC-βH1 cells measured by Western blotting. One representative Western blotting and the densitometric measurements are shown. *I,* apoptosis in EndoC-βH1 cells evaluated by propidium iodide staining. mRNA and protein expression values were normalized by the highest value of each experiment, considered as 1. Results are mean ± S.E. of three to five independent experiments. *, $p < 0.05$, **, $p < 0.01$, and ***, $p < 0.001$ *versus* untreated siCTR; #, $p < 0.05$ and ##, $p < 0.001$, *versus* cytokine-treated siCTR; paired *t* test.

depolarizing the cell membrane from a resting potential of −70 mV to voltages ranging from −50 to +50 mV, and the data obtained were analyzed for charge (*Q*). Rbfox1 KD cells showed a tendency to increase charge (Fig. 6, *J* and *K*). These findings suggest that mild electrophysiological alterations may underlie Rbfox1 KD, but its contribution to the observed phenotype is unclear.

Rbfox1 Regulates Alternative Splicing of Key Genes Controlling Insulin Secretion—To identify Rbfox target genes that might affect insulin release, we re-analyzed a previously published dataset that identified 1,059 Rbfox-regulated AS events in mouse brain (28). Pathway enrichment analysis using IPA (Ingenuity Systems) and DAVID (david.abcc.ncifcrf.gov) software showed that Rbfox-regulated transcripts in brain are enriched in pathways that can affect insulin secretion in beta cells, including cytoskeleton organization, vesicle-mediated transport, and calcium signaling. Three AS events regulated by Rbfox proteins in brain were selected for evaluation in beta cells (Fig. 8). Using two independent siRNAs, we confirmed Rbfox1-

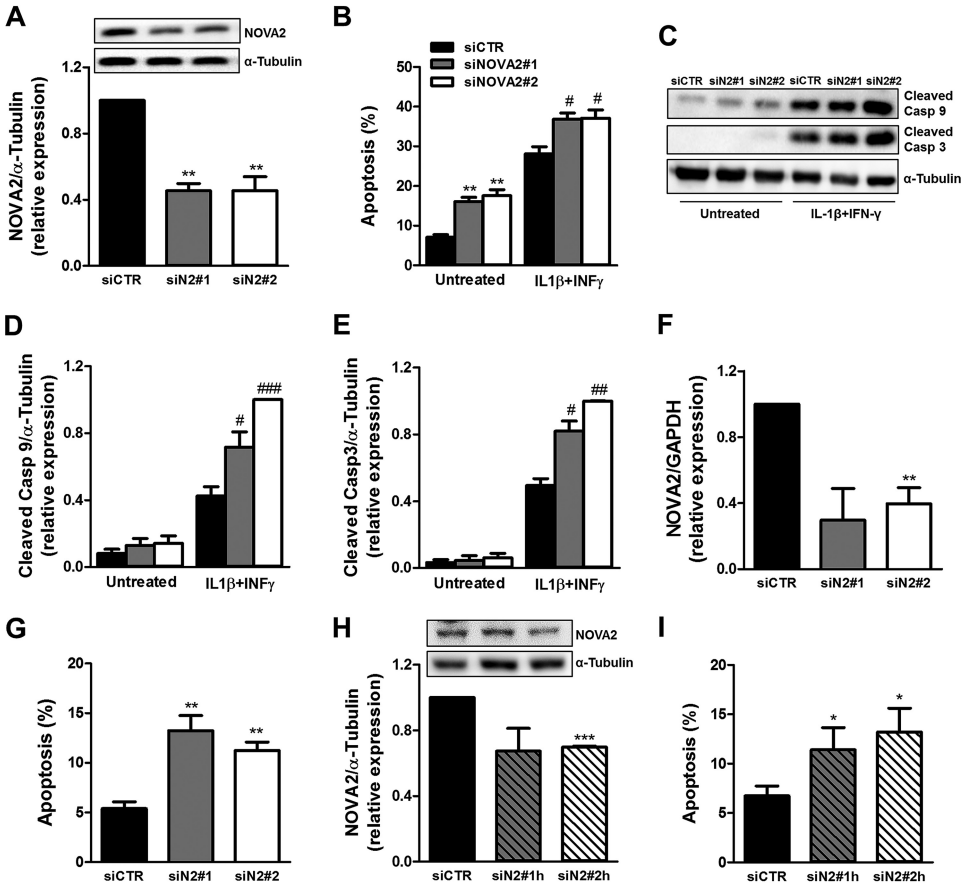

FIGURE 5. **Nova2 knockdown increases apoptosis in pancreatic beta cells.** INS-1E cells (*A–E*), FACS-purified primary rat beta cells (*F* and *G*), and EndoC-βH1 cells (*H* and *I*) were transfected with siCTR or independent siRNAs targeting Nova2 for 48 h and then exposed to the pro-inflammatory cytokines IL-1β + IFN-γ. Cytokine exposure was 24 h for INS-1E cells and 48 h for primary rat beta cells and EndoC-βH1 cells. *A,* protein expression of Nova2 and α-tubulin (used as loading control) in INS-1E cells was measured by Western blotting. One representative blot and densitometric measurements are shown. Apoptosis in INS-1E cells was evaluated by propidium iodide staining (*B*) and by Western blotting for cleaved caspase-9 and cleaved caspase-3 (*C*). Densitometric measurements of cleaved caspase-9 (*D*) and 3 (*E*) are shown. mRNA expression of Nova2 in FACS-purified primary rat beta cells was measured by qRT-PCR and normalized by the housekeeping gene *Gapdh* (*F*), and apoptosis was evaluated by propidium iodide staining (*G*). Protein expression of NOVA2 and α-tubulin (used as loading control) in EndoC-βH1 was measured by Western blotting (*H*). One representative blot and the densitometric measurements are shown. Apoptosis in EndoC-βH1 cells was evaluated by propidium iodide staining (*I*). mRNA and protein expression values were normalized by the highest value of each experiment, considered as 1. Results are mean ± S.E. of three to four independent experiments. *, $p < 0.05$; **, $p < 0.01$; and ***, $p < 0.001$ *versus* untreated siCTR; #, $p < 0.05$; ##, $p < 0.01$; and ###, $p < 0.001$ *versus* cytokine-treated siCTR. *A* and *E–H,* paired *t* test. *B, D,* and *E,* paired *t* test with Bonferroni's correction.

dependent splicing modulation for the actin-remodeling protein gelsolin (*Gsn*) and the voltage-gated calcium channel 1C (*Cacna1c*) (Fig. 8, *A* and *C*). Splicing modulation of the insulin receptor (*Insr*), however, was observed only with one siRNA (Fig. 8*B*). Interestingly, Rbfox1 KD reduced the inclusion of a frameshift cassette exon in *Gsn*, reducing the expression of an isoform predicted to be a target for nonsense-mediated mRNA decay (Fig. 8*A*).

Rbfox1 KD-induced Insulin Secretion Is Mediated by the Actin Remodeling Protein Gelsolin—Gelsolin is a calcium-activated actin-severing protein that plays a positive role in insulin secretion. Gelsolin mediates glucose-dependent actin cytoskeleton depolymerization and interacts with the t-SNARE protein syntaxin 4, facilitating the trafficking, docking, and fusion of insulin granules (29, 30). To evaluate the role of gelsolin in the observed increase in insulin release following Rbfox1 KD, we knocked down in parallel both Rbfox1 and gelsolin in INS-1E cells (Fig. 9). The observed alternative splicing shift following Rbfox1 KD was associated with an increase in gelsolin mRNA expression (Fig. 9*B*), probably secondary to the decrease in the nonsense-mediated mRNA decay-targeted isoform observed in Fig. 8*A*. Knockdown of gelsolin was associated with increased Rbfox1 expression (Fig. 9*A*), indicating a cross-regulation between both genes. Double KD of Rbfox1 and gelsolin prevented the increase in insulin secretion detected after Rbfox1 KD alone (Fig. 9*C*), indicating that the observed phenotype is probably secondary to alterations in cytoskeleton remodeling.

Rbfox1 KD Accelerates Actin Depolymerization Kinetics after Glucose Stimulation—To study whether Rbfox1 KD indeed affects cytoskeleton organization, we evaluated the dynamics of depolymerization of actin filaments following stimulation with glucose using confocal and fluorescence microscopy. Rbfox1 KD did not induce major differences in actin cytoskeleton organization in cells maintained at 0 mM glucose (Fig. 10*A, left panel*), but Rbfox1 KD cells showed less actin stress fibers (F-actin) after stimulation with 17 mM glucose when compared with control cells (Fig. 10*A, right panel*). Actin depoly-

merization was quantified by calculating the ratio between filamentous and globular actin (F/G-actin). Rbfox1-KD cells displayed a faster glucose-induced actin depolymerization when compared with control cells (Fig. 10, *B* and *C*). These differences were more pronounced with siFOX1#2, the siRNA inducing higher levels of Rbfox1 KD and a more extreme phenotype, and were prevented by gelsolin silencing (Fig. 10, *A*–*C*). These findings indicate that the observed increase in insulin secretion following Rbfox KD is secondary to increased gelsolin expression and consequent enhanced actin depolymerization.

Discussion

Beta cells and neurons share many similarities in gene transcription, but whether both cell types present similar AS regulation remains an open question. We presently show that some neuron-enriched splicing regulators are also expressed in pancreatic beta cells where they play a major role in regulating beta

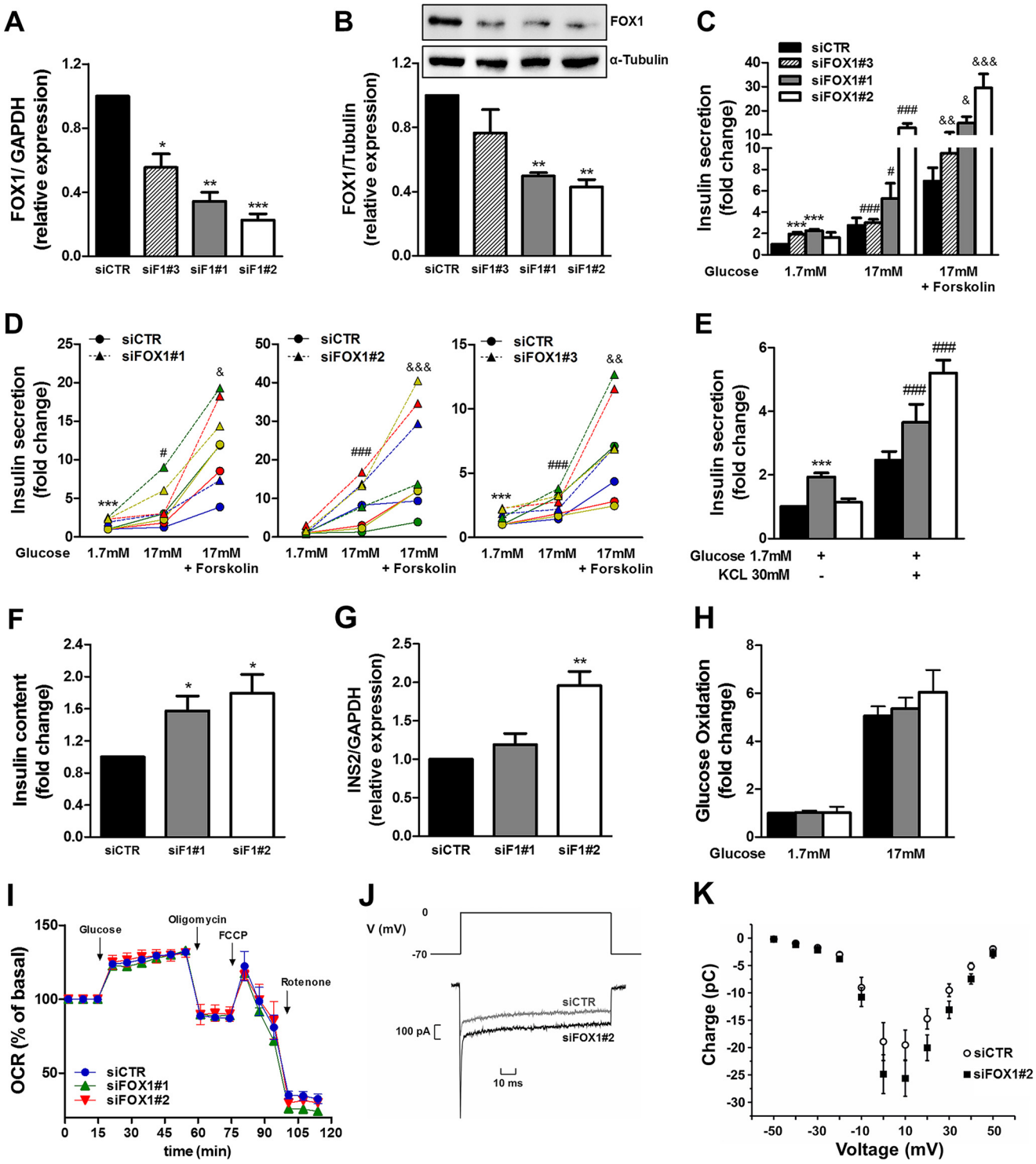

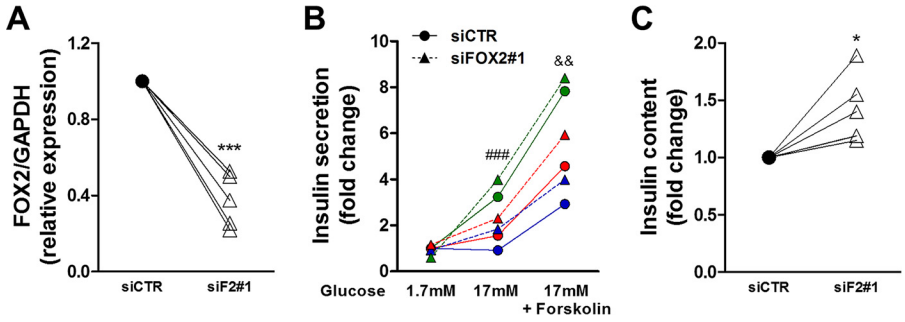

FIGURE 7. **Rbfox2 knockdown increases insulin secretion and content.** INS-1E cells were transfected with siCTR or siFOX2#1 siRNA for 48 h. *A,* mRNA expression of Rbfox2 measured by qRT-PCR and normalized by the housekeeping gene *Gapdh*. mRNA expression values were normalized by the highest value of each experiment, considered as 1. *B,* insulin secretion evaluated by ELISA after 30 min of incubation with 1.7 mM glucose, 17 mM glucose, or 17 mM glucose plus forskolin (20 μM) following Rbfox2 KD. Values are expressed as fold increase as compared with siCTR exposed to 1.7 mM glucose. Individual paired experiments are indicated by the *same color*. *C,* insulin content was evaluated by ELISA. *A* and *C*: *, $p < 0.05$, and ***, $p < 0.001$ *versus* siCTR; paired *t* test. *B*: ###, $p < 0.001$ *versus* siCTR exposed to 17 mM glucose, and &&, $p < 0.01$ *versus* siCTR exposed to 17 mM glucose plus forskolin; paired *t* test with Bonferroni's correction.

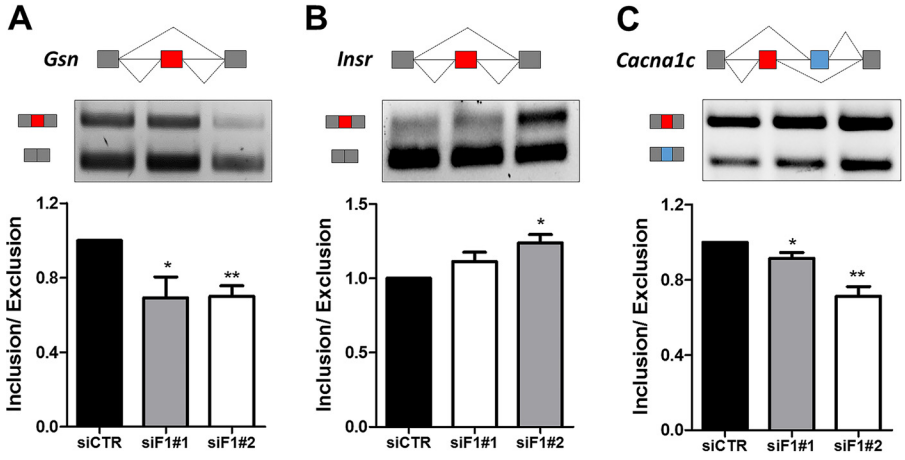

FIGURE 8. **Rbfox1 regulates the alternative splicing of key genes related to pancreatic beta cell function.** *A–C,* representative images of agarose gels showing that Rbfox1 controls alternative splicing of gelsolin (*Gsn*) (*A*), insulin receptor (*Insr*) (*B*), and voltage-gated calcium channel 1C (*Cacna1c*) (*C*) in INS-1E cells. The percentage of inclusion/exclusion of each exon was quantified by densitometry and is shown under the respective gels. Results are mean ± S.E. of five to ten independent experiments. *, $p < 0.05$, and **, $p < 0.01$ *versus* siCTR; paired *t* test.

cell survival and function. Our data analysis identified a cluster of RBPs that are expressed in both brain and in human islets. This cluster includes members of the Elavl, Nova, and Rbfox families, which have been implicated in neuronal physiology and disease (28, 31–35). We found that Elavl4 and Nova2 are required for beta cell survival, and their depletion leads to activation of the intrinsic pathway of apoptosis. In contrast, Rbfox1 and Rbfox2 mostly regulate beta cell function, affecting the insulin secretory capacity but without impact on beta cell viability.

Elavl4 has been implicated in several aspects of mRNA turnover and function, including AS, stability, and translation. Elavl4 acts as a master regulator of neurogenesis, regulating neuronal survival, function, and plasticity (34, 36–38). In pancreatic beta cells Elavl4 has been shown to regulate insulin translation (39), autophagy (40), and lipid synthesis (41). Here we show that Elavl4 also regulates cell survival in beta cells. Intriguingly, Elavl4 silencing increases basal apoptosis but protects against cytokine-induced apoptosis in the three differ-

FIGURE 6. **Rbfox1 knockdown increases insulin secretion.** INS-1E was transfected with siCTR or three independent siRNAs against Rbfox1 (*siFOX1#1, siFOX1#2,* and *siFOX1#3*) for 48 h. *A,* mRNA expression of Rbfox1 measured by qRT-PCR and normalized by the housekeeping gene *Gapdh*. *B,* protein expression of Rbfox1 and α-tubulin (used as loading control) measured by Western blotting. One representative blot and the densitometric measurements are shown. *C,* insulin secretion following Rbfox1 KD evaluated by ELISA after 30 min of incubation with 1.7 mM glucose, 17 mM glucose, or 17 mM glucose plus forskolin (20 μM). *D,* scatter plots showing individual insulin secretion experiments shown in *C*. Individual paired experiments are indicated by the same color. *E,* insulin secretion after 30 min of incubation with 1.7 mM glucose or 1.7 mM glucose plus 30 mM KCl. Insulin secretion values are expressed as fold increase as compared with siCTR exposed to 1.7 mM glucose. *F,* insulin content fold increase as compared with siCTR. *G,* mRNA expression of *Ins2* measured by qRT-PCR and normalized by the housekeeping gene *Gapdh*. *H,* glucose metabolism following exposure to 1.7 or 17 mM glucose after Rbfox1 KD. Values are expressed as fold increase as compared with siCTR exposed to 1.7 mM glucose. *I,* oxygen consumption rates (*OCR*) relative to basal (1.7 mM glucose) following sequential stimulation with glucose (17 mM), oligomycin (5 μM), FCCP (4 μM), and rotenone (1 μM). *J* and *K,* electrophysiological characterization of voltage-gated Ca^{2+} channels following Rbfox1 KD. *J,* example trace of currents evoked by a depolarization from −70 to 0 mV in a single siFOX1#2- (*lower trace*) or siCTR (*upper trace*)-transfected cells. *K,* charge (*Q*)-voltage (*V*) relationship in siFOX1#2- (*black squares*) and siCTR (*white circles*)-transfected cells. Charge is measured as the area enclosed by the curve in *J*. mRNA and protein expression values were normalized by the highest value of each experiment, considered as 1. Results are mean ± S.E. of three to eight independent experiments (*A–I*). *K,* results are mean ± S.E. of 17–20 cells. *A, B, F, G, I,* and *K*: *, $p < 0.05$; **, $p < 0.01$, and ***, $p < 0.001$ *versus* siCTR. *C* and *D*: ***, $p < 0.001$ *versus* siCTR exposed to 1.7 mM glucose; #, $p < 0.05$, and ###, $p < 0.001$ *versus* siCTR exposed to 17 mM glucose; &, $p < 0.05$; &&, $p < 0.01$, and &&&, $p < 0.001$ *versus* siCTR exposed to 17 mM glucose plus forskolin. *F,* ***, $p < 0.001$ *versus* siCTR exposed to 1.7 mM glucose; ###, $p < 0.001$ *versus* siCTR exposed to 30 mM KCl. *A, B, F, G, I,* and *K*: paired *t* test. *C–E* and *H,* paired *t* test with Bonferroni's correction.

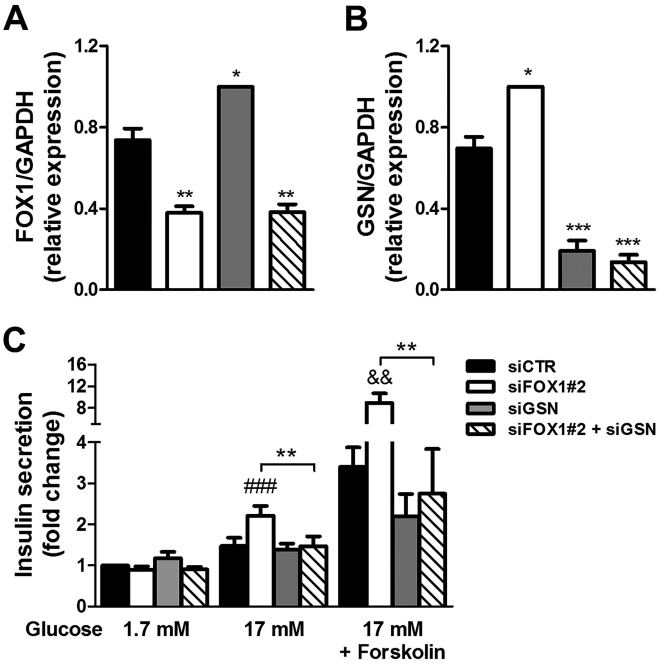

FIGURE 9. **Gelsolin silencing prevents the insulin secretion increase produced by Rbfox1 knockdown.** INS-1E cells were transfected with siCTR, siFOX1#2, siGSN, or siFOX1#2 + siGSN for 48 h. mRNA expression of Rbfox1 (*A*) and gelsolin (*B*) was measured by qRT-PCR and normalized by the housekeeping gene *Gapdh*. mRNA expression values were normalized by the highest value of each experiment, considered as 1. *C*, insulin secretion was evaluated by ELISA after 30 min of incubation with 1.7 mM glucose, 17 mM glucose, or 17 mM glucose plus forskolin (20 μM). Values are expressed as fold increase as compared with siCTR exposed to 1.7 mM glucose. Results are mean ± S.E. of six independent experiments. *A* and *B*, *, $p < 0.05$; **, $p < 0.01$, and ***, $p < 0.001$ *versus* siCTR; paired *t* test. *C*, ###, $p < 0.001$ *versus* siCTR exposed to 17 mM glucose; &&, $p < 0.01$ *versus* siCTR exposed to 17 mM glucose plus forskolin; and **, $p < 0.01$ as indicated by *bars*. Paired *t* test with Bonferroni's correction.

ent models studied. This suggests that Elavl4 may regulate different transcripts and pathways depending on the functional state of the beta cells. Supporting this hypothesis, previous findings indicate that pro-inflammatory cytokines induce changes in the expression of key gene networks for beta cell function and phenotype (42–44) that may be altered by Elavl4 KD. Nevertheless, additional experiments are required to clarify the mechanisms underlying Elavl4 KD.

Nova proteins have been extensively studied in brain where they regulate splicing networks involved in survival, migration, synaptic function, and axon guidance (45–48). We have previously shown that Nova1 controls beta cell function and survival by regulating genes involved in exocytosis, apoptosis, insulin receptor signaling, splicing, and transcription (27). Here we provide additional data showing that Nova2 depletion impairs beta cell survival but not insulin secretion. Increased apoptosis by Nova2 KD may be secondary to up-regulation of the FoxO3A transcription factor and pro-apoptotic protein Bim, as observed previously in Nova1 KD (27). The absence of insulin secretion defects may be explained by differences in targets genes between the Nova paralogs. Alternatively, this may be related to the observed Nova1 up-regulation upon Nova2 silencing, revealing a compensatory mechanism that could decrease physiological perturbations due to changes in splicing pathways. Reciprocal compensatory regulation between RBP paralogs has been previously observed in the Nova and other RBP families (49, 50).

Rbfox1 and Rbfox2 are splicing regulators preferentially expressed in neurons and skeletal muscle and, as shown here, are also found in pancreatic beta cells. In brain, Rbfox proteins regulate a wide range of developmental and synaptic functions. Studies in knock-out mice and in human neural stem cells showed that Rbfox1 regulates neuronal development and excitability (32, 51), whereas Rbfox2 affects neuron migration in the cerebellum (52). In addition, mutations in Rbfox1 are found in patients with epilepsy, spinocerebellar ataxia, and autism spectrum disorders (53–56). In skeletal muscle, the absence of Rbfox1 leads to abnormal myofibrillar structure and impaired muscle function (57). Our data indicate that Rbfox proteins also play an important role in regulating insulin exocytosis in beta cells. Proper beta cell function relies on efficient insulin storage and secretion in response to increased blood glucose levels. Glucose-stimulated insulin secretion is modulated by a number of factors, including glucose metabolism, calcium signaling, and cytoskeleton remodeling (58–61). We observed that both Rbfox1 and Rbfox2 silencing increase insulin secretion and content. The similar phenotype observed for Rbfox1 and Rbfox2 KD suggests that both RBPs regulate overlapping sets of transcripts in beta cells. This is in agreement with previous studies showing that Rbfox proteins bind to the same UGCAUG motif due to the presence of a common RNA binding domain (28, 32, 62). Functional analysis of the role of Rbfox proteins in beta cells (present data) indicates that Rbfox depletion increases the insulin secretory capacity by affecting actin depolymerization kinetics following glucose stimulation. Thus, Rbfox1 regulates the splicing of the actin remodeling protein gelsolin, modulating the expression of a non-productive isoform and thus affecting overall gelsolin expression. Inhibition of gelsolin expression prevented the Rbfox1 KD-induced insulin secretion increase and actin cytoskeleton alterations. Gelsolin enhances insulin secretion by mediating glucose-dependent actin cytoskeleton remodeling and by interacting with t-SNARE proteins, thus favoring insulin granule exocytosis (29, 30). In line with the present findings, Rbfox1 targets in brain and muscle are enriched in genes involved in cytoskeleton organization and actin filament-based processes (28, 57). We cannot exclude, however, that other Rbfox targets (such as calcium channels) also contribute to the observed phenotype.

In conclusion, these data indicate that pancreatic beta cells express neuron-enriched RBPs that control beta cell function and survival, suggesting that neurons and beta cells share common splicing regulatory programs. Splicing programs provide a highly interconnected regulatory layer to control gene expression and promote cell specialization in differentiated tissues. These findings provide a better understanding on how AS regulates beta cell survival and function, and they point the way to identify the role for AS in beta cell dysfunction in diabetes.

Experimental Procedures

RNA-sequencing Data Visualization—To analyze the expression pattern of splicing factors in human islets and in 16 other human tissues, we used a previously published RNA-sequencing

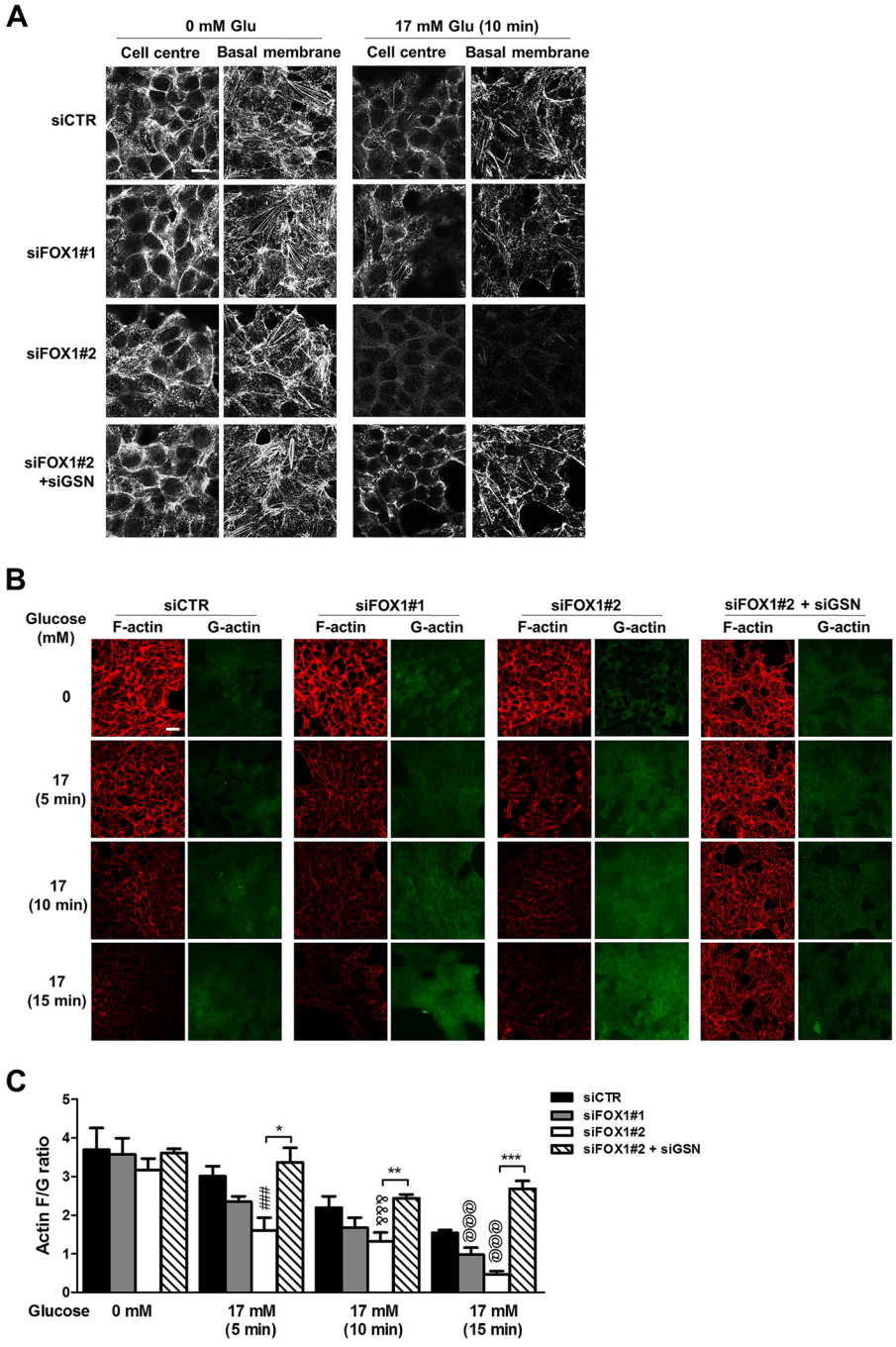

FIGURE 10. **Rbfox1 knockdown accelerates actin depolymerization dynamics after glucose stimulation, a phenomenon prevented by gelsolin silencing.** *A*, confocal microscopy images of actin cytoskeleton in INS-1E cells following incubation at 0 or 17 mM glucose during 10 min. Cells were transfected with siCTR, siFOX1#1, siFOX1#2, or siFOX1#2 + siGSN for 48 h. *B* and *C*, quantification of actin depolymerization following glucose stimulation by the F/G ratio in INS-1E cells. Atto 550-phalloidin (*red*) staining actin filaments and DNase I-Alexa 488 (*green*) staining globular actin were used to quantify the emitted fluorescence, and calculation of the ratio is shown in *C*. ###, $p < 0.001$ *versus* siCTR exposed to 17 mM glucose during 5 min; &&&, $p < 0.001$ *versus* siCTR exposed to 17 mM glucose during 10 min; @@@, $p < 0.001$ *versus* siCTR exposed to 17 mM glucose during 15 min; *, $p < 0.05$; **, $p < 0.01$, and ***, $p < 0.001$ as indicated by *bars*. Paired *t* test with Bonferroni's correction. *Scale bars,* 10 μm (*A*) and 20 μm (*B*).

dataset (24) and the Illumina BodyMap 2.0 dataset (GEO: GSE30611). A list of human splicing factors was manually curated by combining the SpliceAid-F database (63) with other RBPs that have been described in the literature or in other databases as splicing regulators. Log transformed reads per kb/million mapped reads (RPKM) gene expression values were used to generate a two-way hierarchical clustering heat map using Gene Pattern modules (64) with default parameters (not centered, not normalized).

Culture of Rat INS-1E Cells, FACS-purified Primary Rat Beta Cells, Human EndoC-βH1 Cells, and Human Islets—Rat insulin-producing INS-1E cells, kindly provided by Dr. C. Wollheim (University of Geneva, Geneva, Switzerland), were cultured in RPMI 1640 GlutaMAX-I medium (Invitrogen) as described previously (65).

Primary beta cells were obtained from male Wistar rats (Charles River Laboratories, Brussels, Belgium). Rats were

TABLE 1

Characteristics of the organ donors and human islet preparations used for RNA-sequencing and independent confirmation

The abbreviations used are as follows: F, female; M, male; BMI, body mass index; CVD, cardiovascular disease; CH, cerebral hemorrhage; PAE, post-anoxic encephalopathy. Purity indicates the percentage of beta cells in the human islet preparations as determined by immunostaining for insulin.

	Gender	Age	BMI	Cause of death	Purity
		years	*kg/m²*		*%*
Islets for RNA-sequencing					
ID1	F	77	24	Trauma	45
ID2	F	46	23	CVD	60
ID3	F	79	28	Trauma	61
ID4	M	36	26	CVD	62
ID5	M	77	25	CVD	62
Islets for qPCR					
ID6	F	75	29	CVD	49
ID7	M	79	25	CH	48
ID8	M	44	28	PAE	59

housed and used according to the guidelines of the Belgian Regulations for Animal Care, with the approval by the local Ethical Committee. Pancreatic islets were isolated by collagenase digestion, handpicked, and dissociated into single cells by mechanical and enzymatic dispersion, and beta cells were purified by FACS sorting as described previously (66). Purified beta cells were cultured in Ham's F-10 medium containing 10 mM glucose, 2 mM GlutaMAX, 0.5% BSA, 50 μM isobutylmethylxanthine, 50 units/ml penicillin and 50 μg/ml streptomycin, and 5% heat-inactivated fetal bovine serum (FBS, Gibco Life Technologies, Inc.).

Human insulin-producing EndoC-βH1 cells, kindly provided by Dr. R. Sharfmann (Institut Cochin, Université Paris Descartes, Paris, France), were grown on plates coated with Matrigel/fibronectin (100 and 2 μg/ml, respectively, Sigma), and cultured in DMEM as described previously (67, 68).

Human islets from eight non-diabetic donors were isolated in Pisa, Italy, using collagenase digestion and density gradient purification (69). The donors (four men and four women) were age 64 $\pm$ 18 years and had a body mass index of 26 $\pm$ 2 kg/m^2. Cause of death was cardiovascular disease in four cases, trauma in two cases, cerebral hemorrhage in one case, and post-anoxic encephalopathy in one case. Beta cell purity, as evaluated by immunofluorescence for insulin using a specific anti-insulin antibody, was 56 $\pm$ 7% (Table 1). Islets were cultured at 6.1 mmol/liter glucose as described previously (24, 70).

Cell Treatment—INS-1E and EndoC-βH1 cells were exposed to the following cytokine concentrations, based on previous dose-response experiments performed by our group (65, 68): recombinant human IL-1β (R&D Systems, Abingdon, UK) 10 units/ml for INS-1E cells or primary rat beta cells and 50 units/ml for EndoC-βH1 cells; recombinant rat IFN-γ (R&D Systems) 100 or 500 units/ml for INS-1E cells or primary rat beta cells, respectively; and human IFN-γ (PeproTech, London, UK) 1000 units/ml for EndoC-βH1 cells. Lower cytokine concentrations and shorter time intervals were used in INS-1E and FACS-purified rat beta cells experiments because rat beta cells are more sensitive to cytokine-induced damage than human beta cells (71).

Infection with Recombinant Adenoviruses—To overexpress REST in INS-1E cells, we used a recombinant adenovirus containing the full-length cDNA of human *REST* kindly provided by Dr. F. Allagnant (University of Lausanne, Lausanne, Switzerland) (13). After 48 h of pre-culture, INS-1E cells were infected with the recombinant adenovirus encoding REST or with a control adenovirus encoding *Renilla* luciferase (72). Cells were infected for 24 h at 37 °C at an m.o.i. of 10 and collected for mRNA extraction.

RNA Interference—The small interfering RNAs (siRNAs, Life Technologies, Inc.) targeting rat and human genes used in this study are described in Table 2. Allstar Negative Control siRNA (siCTR) (Qiagen) was used as negative control in all experiments. This siCTR does not affect beta cell gene expression, function, or viability (73). Transient transfection was performed using 30 nM siRNA and Lipofectamine RNAiMAX lipid reagent (Invitrogen-Life Technologies, Inc.) as described previously (73). After 16 h of transfection, cells were cultured for a 48-h recovery period before exposure to cytokines.

Assessment of Cell Viability—The percentage of apoptotic, necrotic, and viable cells was determined by fluorescence microscopy after 15 min of incubation with the DNA-binding dyes propidium iodide (5 mg/ml) and Hoechst 33342 (10 mg/ml) (Sigma). A minimum of 600 cells was counted for each experimental condition by two independent observers, one of them unaware of the sample identity. The agreement between researchers was >90%. Apoptosis was further confirmed in some experiments by cleavage of caspase-3 and -9 by Western blotting (see below).

mRNA Extraction, RT-PCR, and qRT-PCR—Poly(A)$^+$-RNA was isolated from INS-1E cells, primary rat β-cells, EndoC-βH1 cells, and human islets using the Dynabeads mRNA DIRECT kit (Invitrogen) and reverse-transcribed as described previously (74). cDNAs from 14 normal human tissues (adipose, brain, colon, heart, kidney, liver, lung, lymph node, pancreas, skeletal muscle, small intestine, spleen, stomach, and testes) were obtained from BioChain Laboratories (San Francisco, CA). The real time PCR amplification reaction was performed using SYBR Green (Bio-Rad, Nazareth Eke, Belgium) and compared with a standard curve as described (75). Expression values were corrected for the housekeeping genes glyceraldehyde-3-phosphate dehydrogenase (*Gapdh*) for rat beta cells or β-actin for human cells. Expression of these housekeeping genes is not modified under the present experimental conditions (70). The primers used in this study are detailed in Table 3.

Insulin Secretion—To assess insulin secretion, INS-1E cells were pre-incubated for 1 h in glucose-free RPMI 1640 Gluta MAX-I medium (Life Technologies, Inc.) followed by incubation with Krebs-Ringer solution for 30 min. Cells were then exposed to 1.7, 17, or 17 mM glucose plus 20 μM forskolin or to 30 mM KCl during 30 min. Insulin release and insulin content were measured using the rat insulin ELISA kit (Mercodia, Uppsala, Sweden) in cell-free supernatants and acid/ethanol-extracted cell lysates, respectively. Results were normalized by total protein content, determined by the Bradford dye method.

Glucose Oxidation—D-[U-^{14}C]Glucose (specific activity, 300 mCi/mM; concentration, 1 mCi/ml (PerkinElmer Life Sciences) was used to assess glucose oxidation in control and Rbfox1 KD

TABLE 2
Sequences of siRNAs used to knock down gene/protein expression

Gene	Species	Name	Supplier	Sequence
None		siCTR All-stars Negative control siRNA	Qiagen, Venlo, The Netherlands	Not provided
Elavl4	*Rattus norvegicus*	siELAVL4#1 silencer select siRNAi	Invitrogen, Paisley, UK	5′ GAGGCAUUGGUGAAAUCGAATT 3′ 5′ UUCGAUUUCACCAAUGCUCCC 3′
Elavl4	*R. norvegicus*	siELAVL4#2 silencer select siRNAi	Invitrogen, Paisley, UK	5′ GAUUCAGGCUGGACAAUUUTT 3′ 5′ AAAUUGUCCAGCCUGAAUCTT 3′
Nova2	*R. norvegicus*	siNOVA2#1 stealth select siRNAi	Invitrogen, Paisley, UK	5′ AGGUCCGAGAAAUCCCUCAAGCGAU 3′ 5′ AUCGCUUGAGGGAUUUCUCGGACCU 3′
Nova2	*R. norvegicus*	siNOVA2#1 stealth select siRNAi	Invitrogen, Paisley, UK	5′ CGGGAGCCACCAUCAAGCUAUCUAA 3′ 5′ UUAGAUAGCUUGAUGGUGGCUCCCG 3′
Rbfox1	*R. norvegicus*	siFOX1#1 silencer select siRNAi	Invitrogen, Pasley, UK	5′ GAUUUGGUUUCGUAACUUUTT 3′ 5′ AAAGUUACGAAACCAAAUCCC 3′
Rbfox1	*R. norvegicus*	siFOX1#2 silencer select siRNAi	Invitrogen, Paisley, UK	5′ CGAGGUUAAUAAUGCGACATT 3′ 5′ UGUCGCAUUAUUAACCUCGAT 3′
Rbfox1	*R. norvegicus*	siFOX1#3 silencer select siRNAi	Invitrogen, Paisley, UK	5′ GCGGUGUUGUUACCAGGATT 3′ 5′ UCCUGGUAAACAACACCGCCA 3′
Rbfox2	*R. norvegicus*	siFOX2#1 silencer select siRNAi	Invitrogen, Paisley, UK	5′ AGAAGAUGGUCACACCAUATT 5′ UAUGGUGUGACCAUCUUCUTG 3′
Gsn	*R. norvegicus*	siGSN FlexiTube siRNA	Qiagen, Hilden, Germany	5′ CAUCACUGUCGUUAGGCAATT 3′ 5′ UUGCCUAACGACAGUGAUGGG 3′
ELAVL4	*Homo sapiens*	siELAVL4#1h silencer select siRNAi	Invitrogen, Paisley, UK	5′ CAAUUACCAUUGAUGGAUTT 3′ 5′ AUUCCAUCAAUGGUAAUUGGG 3′
NOVA2	*H. sapiens*	siNOVA2#1h stealth select siRNAi	Invitrogen, Paisley, UK	5′ GACAGAGCCAAGCAGGCCAAGCUGA 3′ 5′ UCAGCUUGGCCUGCUUGGCUCUGUC 3′
NOVA2	*H. sapiens*	siNOVA2#2h stealth select siRNAi	Invitrogen, Paisley, UK	5′ UGCUGGCCAUCAGCACGGCGCUUAA 3′ 5′ UUAAGCGCCGUGCUGAUGGCCAGCA 3′

TABLE 3
Primers sequences used for real time and splicing analyses
The abbreviations used are as follows: qRT, primers used for real time qRT-PCR; SPL, primers used to analyze splicing variants.

Target gene	Application	Forward (5′–3′)	Reverse (5′–3′)
Rat			
Gapdh	qRT	AGTTCAACGGCACAGTCAAG	TACTCAGCACCAGCATCACC
Elavl4	qRT	CCAAAGGATGCAGAGAAAGC	GGGAAGGCCACTAACGTACA
Nova2	qRT	CTCAATCATCGGCAAAGGTG	GGCTCTGTCGGGGTTCATC
Rbfox1	qRT	GGGCGAGGAGGGGAAGGGAG	GTGCGCACTGTAGCAGGCCA
Rbfox2	qRT	GCAAATGGCTGGAAGTTAAGC	CATTGCCTAGGGACACATCA
Rest	qRT	TGAAAAGTCCGTCAAAGCAG	GCACATCCATCTCTTTCACCT
Elavl1	qRT	TGACAAACGGTCTGAAGCAG	CCTGAATCTCTGTGCCTGGT
Nova1	qRT	GGAGCAGTCAGGGGCTTGGG	TGAGACAGCTGCCACTCTGTGGA
Ins2	qRT	TGACCAGCTACAGTCGGAAA	GTTGCAGTAGTTCTCCAGTTGG
Gsn	qRT	CTTTGTTTGGAAAGGCAAGC	GGGGTACTGCATCTTGGAGA
Cacna1c	SPL	AGTGATCCCTGGAATGTTTTTG	AGGACTTGATGAAGGTCCACAG
Insr	SPL	TGCACAACGTGGTTTTTGTT	TCTCTTCTGGGGAGTCCTGA
Gsn	SPL	ATGGCTCCGTATTGCTCCT	AACTTCTCCACACGCCAGAT
Human			
ACTB	qRT	GCGCGGCTACAGCTTCA	CTTAATGTCACGCACGATTTCC
ELAVL4	qRT	GCTACCCAGGTCCACTTCAC	GGATGTTCATTCCCACAAGG
NOVA2	qRT	CCATCAAGCTCTCCAAGTCC	GGGATTTCTCGGACCTTCTC

cells exposed to different glucose concentrations as described (76). The rate of glucose oxidation was expressed as pmol/10^5 cells·120 min^{-1} and normalized by the glucose oxidation observed in control cells under low glucose concentrations.

Mitochondrial Respiration—Oxygen consumption rates were measured by the XFp Extracellular Flux Analyzer (Seahorse Bioscience, North Billerica, MA). INS-1E cells were pre-incubated for 1 h in assay medium containing 1.7 mM glucose at 37 °C in air after which respiration was measured following sequential injections of 17 mM glucose, 5 μM oligomycin, 4 μM FCCP, and 1 μM rotenone as described (77).

Electrophysiological Measurements—Experiments were conducted on single INS-1E cells. Patch pipettes were pulled from borosilicate glass capillaries and then coated with sticky wax (Kemdent, Wiltshire, UK) and fire-polished. Patch pipettes had a resistance of 3–6 megohms when filled with the pipette solution specified below. All recordings were conducted at 32–34 °C using an EPC-9 patch clamp amplifier and Pulse software version 8.80 (HEKA Electronics, Lambrecht, Germany) without visualization of the transfected cells. Standard whole-cell configurations of the patch clamp technique were used, and Ca^{2+} currents were evoked by depolarizing the cell membrane from a resting potential of −70 mV to voltages ranging from −50 to +50 mV (78). Standard extracellular solution consisted of the following (in mM): 118 NaCl, 20 tetraethylammonium chloride (to block K^+ currents), 5.6 KCl, 2.6 $CaCl_2$, 1.2 $MgCl_2$, 5 glucose, and 5 HEPES (pH 7.4 using NaOH), and the pipette solution consisted of the following (in mM): 125 cesium glutamate, 10 NaCl, 10 CsCl, 1 $MgCl_2$, 0.05 EGTA, 3 Mg-ATP, 5 HEPES (pH 7.15 using CsOH) and 0.1 cAMP. To exclude any depolarization-induced Na^+ currents from the analysis, charge (Q) was measured 1.4 ms after the onset until the end of the depolarization.

Actin Filaments Immunofluorescence—INS-1E cells were cultured on glass slides coated with Matrigel-fibronectin (100 and 2 μg/ml, respectively; Sigma) and transfected with control or Rbfox1 siRNAs for 48 h. Following the same protocol used to analyze insulin secretion, cells were incubated for 1 h in

TABLE 4
Antibodies and fluorescent labels used for Western blotting and immunofluorescence

Antibody	Company	Reference	Dilution
Elavl4 (rabbit)	Abcam, Cambridge, UK	ab96474	1:1000
Nova2 (rabbit)	MBL, Ina, Japan	RN044PW	1:500
Rbfox1 (rabbit)	Abcam, Cambridge, UK	Ab154490	1:1000
Cleaved caspase 3 (rabbit)	Cell Signaling, Danvers, MA	9661S	1:1000
Cleaved caspase 9 (rabbit)	Cell Signaling, Danvers, MA	9507	1:1000
Tubulin (mouse)	Sigma, Bornem, Belgium	T5168	1:10,000
HRP-conjugated anti-rabbit IgG	Jackson ImmunoResearch	711-036-152	1:10,000
HRP-conjugated anti-mouse IgG	Jackson ImmunoResearch	711-036-150	1:10,000
Deoxyribonuclease I-Alexa Fluor 488	Life Technologies, Inc.	D12371	1:500
Atto 550-phalloidin	Sigma, Bornem, Belgium	19083	1:500

glucose-free RPMI 1640 GlutaMAX-I medium followed by 30-min incubation in glucose-free Krebs-Ringer solution. Cells were then exposed to 17 mM glucose at different time points (5, 10, and 15 min) and immediately after fixed in 4% paraformaldehyde for 10 min. The cells were then washed with PBS and permeabilized in Triton X-100 0.25% for 3 min. Slides were then blocked using 3% BSA and incubated at room temperature in sequential order with deoxyribonuclease I-Alexa Fluor 488 conjugate (Life Technologies, Inc.) and Atto 550-phalloidin (Sigma) to specifically stain G-actin (globular) and F-actin (filaments), respectively. Nuclei were stained with Hoechst 33342. Cells were visualized under a Zeiss Axiovert 200 inverted fluorescence microscope (Carl Zeiss, Zaventem, Belgium) at ×40. Images were acquired and processed using the AxioVision LE64 software (Carl Zeiss). For F/G actin quantification, all samples were processed together to avoid changes in the image intensity. Exposure was locked to 100 ms to obtain all acquisitions under the same conditions. ImageJ software was used to measure the pixel intensity of both channels using the whole field of every image. These intensities were used to calculate the F/G actin ratio.

Confocal Imaging—Cells samples were observed under a Zeiss LSM780 inverted confocal microscope using ×40/1.1 water objective. Z-stacks of images were acquired sequentially and processed using Zen2010 software (Carl Zeiss).

Western Blotting—For Western blotting, cells were washed with cold PBS and lysed using Laemmli Sample Buffer. Total protein was extracted and resolved by 8–12% SDS-PAGE, transferred to a nitrocellulose membrane, and immunoblotted with the specific antibodies for the protein of interest (Table 4) as described (79). Protein signal was visualized using chemiluminescence Supersignal (Pierce). ChemiDoc MP system and Image Lab software version 4.1 (Bio-Rad, Perth, UK) were used for image acquisition and densitometric analysis of the blots. The software allows automatic exposure optimization, ensuring the best use of the dynamic range. Saturation or overexposure is avoided by overriding the images that displayed pixels in red. Densitometric values were corrected by the housekeeping protein α-tubulin as loading control, after background subtraction.

Statistical Analysis—Data are showed as means ± S.E. or as independent data points. Significant differences between experimental conditions were assessed by a paired Student's *t* test. In case of multiple *t* test comparisons, the Bonferroni correction was applied as indicated (80). p values < 0.05 were considered statistically significant.

Author Contributions—J. J.-M. and T. H. R. designed the study, researched the data, performed analyses, and wrote the manuscript. O. V., E. L-M., A. W., J.-V. T., L. A. B., T. R. N., T. C. N., M. I. A., J. L. S. E., and L. E. researched the data. P. M. contributed with material and critically revised the manuscript. D. L. E. designed the study, analyzed the data, and wrote the manuscript. All co-authors read the final version of the manuscript. D. L. E. and J. J.-M. are the guarantors of this work and, as such, had full access to all the data in the study and take responsibility for the integrity of the data and the accuracy of the data analyses.

Acknowledgments—We thank Isabelle Millard, Anyishaï Musuaya, Nathalie Pachera, Michaël Pangerl, and Anna-Maria Veljanovska Ramsay for expert technical assistance. We are grateful to Christine Dubois and to the Flow Cytometry Facility of the Erasmus campus of the Université Libre de Bruxelles for the FACS purification of beta cells and to Prof. Dr. Jean-Marie Vanderwinden of the Light Microscopy Facility (LiMiF) at Université Libre de Bruxelles for advice and support for the confocal imaging.

References

1. Arntfield, M. E., and van der Kooy, D. (2011) Beta-cell evolution: how the pancreas borrowed from the brain. The shared toolbox of genes expressed by neural and pancreatic endocrine cells may reflect their evolutionary relationship. *Bioessays* **33,** 582–587
2. Regazzi, R., Wollheim, C. B., Lang, J., Theler, J. M., Rossetto, O., Montecucco, C., Sadoul, K., Weller, U., Palmer, M., and Thorens, B. (1995) VAMP-2 and cellubrevin are expressed in pancreatic beta-cells and are essential for Ca^{2+}-but not for GTPγS-induced insulin secretion. *EMBO J.* **14,** 2723–2730
3. Sadoul, K., Lang, J., Montecucco, C., Weller, U., Regazzi, R., Catsicas, S., Wollheim, C. B., and Halban, P. A. (1995) SNAP-25 is expressed in islets of Langerhans and is involved in insulin release. *J. Cell Biol.* **128,** 1019–1028
4. Leung, Y. M., Kwan, E. P., Ng, B., Kang, Y., and Gaisano, H. Y. (2007) SNAREing voltage-gated K^+ and ATP-sensitive K^+ channels: tuning beta-cell excitability with syntaxin-1A and other exocytotic proteins. *Endocr. Rev.* **28,** 653–663
5. Henquin, J. C., and Meissner, H. P. (1984) The ionic, electrical, and secretory effects of endogenous cyclic adenosine monophosphate in mouse pancreatic B cells: studies with forskolin. *Endocrinology* **115,** 1125–1134
6. Jensen, J. (2004) Gene regulatory factors in pancreatic development. *Dev. Dyn.* **229,** 176–200
7. Hartenstein, V., and Stollewerk, A. (2015) The evolution of early neurogenesis. *Dev. Cell.* **32,** 390–407
8. van Arensbergen, J., García-Hurtado, J., Moran, I., Maestro, M. A., Xu, X., Van de Casteele, M., Skoudy, A. L., Palassini, M., Heimberg, H., and Ferrer, J. (2010) Derepression of Polycomb targets during pancreatic organogenesis allows insulin-producing beta-cells to adopt a neural gene activity program. *Genome Res.* **20,** 722–732

9. Devaskar, S. U., Giddings, S. J., Rajakumar, P. A., Carnaghi, L. R., Menon, R. K., and Zahm, D. S. (1994) Insulin gene expression and insulin synthesis in mammalian neuronal cells. *J. Biol. Chem.* **269,** 8445–8454
10. Hori, Y., Gu, X., Xie, X., and Kim, S. K. (2005) Differentiation of insulin-producing cells from human neural progenitor cells. *PLoS Med.* **2,** e103
11. Atouf, F., Czernichow, P., and Scharfmann, R. (1997) Expression of neuronal traits in pancreatic beta cells. Implication of neuron-restrictive silencing factor/repressor element silencing transcription factor, a neuron-restrictive silencer. *J. Biol. Chem.* **272,** 1929–1934
12. Thiel, G., Ekici, M., and Rössler, O. G. (2015) RE-1 silencing transcription factor (REST): a regulator of neuronal development and neuronal/endocrine function. *Cell Tissue Res.* **359,** 99–109
13. Martin, D., Tawadros, T., Meylan, L., Abderrahmani, A., Condorelli, D. F., Waeber, G., and Haefliger, J. A. (2003) Critical role of the transcriptional repressor neuron-restrictive silencer factor in the specific control of connexin36 in insulin-producing cell lines. *J. Biol. Chem.* **278,** 53082–53089
14. Martin, D., Allagnat, F., Chaffard, G., Caille, D., Fukuda, M., Regazzi, R., Abderrahmani, A., Waeber, G., Meda, P., Maechler, P., and Haefliger, J. A. (2008) Functional significance of repressor element 1 silencing transcription factor (REST) target genes in pancreatic beta cells. *Diabetologia* **51,** 1429–1439
15. Martin, D., Kim, Y. H., Sever, D., Mao, C. A., Haefliger, J. A., and Grapin-Botton, A. (2015) REST represses a subset of the pancreatic endocrine differentiation program. *Dev. Biol.* **405,** 316–327
16. Chen, M., and Manley, J. L. (2009) Mechanisms of alternative splicing regulation: insights from molecular and genomics approaches. *Nat. Rev. Mol. Cell Biol.* **10,** 741–754
17. Zheng, S., and Black, D. L. (2013) Alternative pre-mRNA splicing in neurons: growing up and extending its reach. *Trends Genet.* **29,** 442–448
18. Raj, B., and Blencowe, B. J. (2015) Alternative splicing in the mammalian nervous system: recent insights into mechanisms and functional roles. *Neuron* **87,** 14–27
19. Licatalosi, D. D., and Darnell, R. B. (2006) Splicing regulation in neurologic disease. *Neuron* **52,** 93–101
20. Glatt, S. J., Cohen, O. S., Faraone, S. V., and Tsuang, M. T. (2011) Dysfunctional gene splicing as a potential contributor to neuropsychiatric disorders. *Am. J. Med. Genet. B. Neuropsychiatr. Genet.* **156,** 382–392
21. Grabowski, P. J., and Black, D. L. (2001) Alternative RNA splicing in the nervous system. *Prog. Neurobiol.* **65,** 289–308
22. Lee, C. J., and Irizarry, K. (2003) Alternative splicing in the nervous system: an emerging source of diversity and regulation. *Biol. Psychiatry* **54,** 771–776
23. Li, Q., Lee, J. A., and Black, D. L. (2007) Neuronal regulation of alternative pre-mRNA splicing. *Nat. Rev. Neurosci.* **8,** 819–831
24. Eizirik, D. L., Sammeth, M., Bouckenooghe, T., Bottu, G., Sisino, G., Igoillo-Esteve, M., Ortis, F., Santin, I., Colli, M. L., Barthson, J., Bouwens, L., Hughes, L., Gregory, L., Lunter, G., Marselli, L., *et al.* (2012) The human pancreatic islet transcriptome: expression of candidate genes for type 1 diabetes and the impact of pro-inflammatory cytokines. *PLoS Genet.* **8,** e1002552
25. Nogueira, T. C., Paula, F. M., Villate, O., Colli, M. L., Moura, R. F., Cunha, D. A., Marselli, L., Marchetti, P., Cnop, M., Julier, C., and Eizirik, D. L. (2013) GLIS3, a susceptibility gene for type 1 and type 2 diabetes, modulates pancreatic beta cell apoptosis via regulation of a splice variant of the BH3-only protein Bim. *PLoS Genet.* **9,** e1003532
26. Juan-Mateu, J., Villate, O., and Eizirik, D. L. (2016) Mechanisms in endocrinology: alternative splicing: the new frontier in diabetes research. *Eur. J. Endocrinol.* **174,** R225–R238
27. Villate, O., Turatsinze, J. V., Mascali, L. G., Grieco, F. A., Nogueira, T. C., Cunha, D. A., Nardelli, T. R., Sammeth, M., Salunkhe, V. A., Esguerra, J. L., Eliasson, L., Marselli, L., Marchetti, P., and Eizirik, D. L. (2014) Nova1 is a master regulator of alternative splicing in pancreatic beta cells. *Nucleic Acids Res.* **42,** 11818–11830
28. Weyn-Vanhentenryck, S. M., Mele, A., Yan, Q., Sun, S., Farny, N., Zhang, Z., Xue, C., Herre, M., Silver, P. A., Zhang, M. Q., Krainer, A. R., Darnell, R. B., and Zhang, C. (2014) HITS-CLIP and integrative modeling define the Rbfox splicing-regulatory network linked to brain development and autism. *Cell. Rep.* **6,** 1139–1152
29. Tomas, A., Yermen, B., Min, L., Pessin, J. E., and Halban, P. A. (2006) Regulation of pancreatic beta-cell insulin secretion by actin cytoskeleton remodelling: role of gelsolin and cooperation with the MAPK signalling pathway. *J. Cell Sci.* **119,** 2156–2167
30. Kalwat, M. A., Wiseman, D. A., Luo, W., Wang, Z., and Thurmond, D. C. (2012) Gelsolin associates with the N terminus of syntaxin 4 to regulate insulin granule exocytosis. *Mol. Endocrinol.* **26,** 128–141
31. Yang, Y. Y., Yin, G. L., and Darnell, R. B. (1998) The neuronal RNA-binding protein Nova-2 is implicated as the autoantigen targeted in POMA patients with dementia. *Proc. Natl. Acad. Sci. U.S.A.* **95,** 13254–13259
32. Gehman, L. T., Stoilov, P., Maguire, J., Damianov, A., Lin, C. H., Shiue, L., Ares, M, Jr., Mody, I., and Black, D. L. (2011) The splicing regulator Rbfox1 (A2BP1) controls neuronal excitation in the mammalian brain. *Nat. Genet.* **43,** 706–711
33. Calarco, J. A., Zhen, M., and Blencowe, B. J. (2011) Networking in a global world: establishing functional connections between neural splicing regulators and their target transcripts. *RNA* **17,** 775–791
34. Bronicki, L. M., and Jasmin, B. J. (2013) Emerging complexity of the HuD/ELAVl4 gene; implications for neuronal development, function, and dysfunction. *RNA* **19,** 1019–1037
35. Hayashi, S., Yano, M., Igarashi, M., Okano, H. J., and Okano, H. (2015) Alternative role of HuD splicing variants in neuronal differentiation. *J. Neurosci. Res.* **93,** 399–409
36. Akamatsu, W., Fujihara, H., Mitsuhashi, T., Yano, M., Shibata, S., Hayakawa, Y., Okano, H. J., Sakakibara, S., Takano, H., Takano, T., Takahashi, T., Noda, T., and Okano, H. (2005) The RNA-binding protein HuD regulates neuronal cell identity and maturation. *Proc. Natl. Acad. Sci. U.S.A.* **102,** 4625–4630
37. Perrone-Bizzozero, N., and Bird, C. W. (2013) Role of HuD in nervous system function and pathology. *Front. Biosci.* **5,** 554–563
38. Wang, F., Tidei, J. J., Polich, E. D., Gao, Y., Zhao, H., Perrone-Bizzozero, N. I., Guo, W., and Zhao, X. (2015) Positive feedback between RNA-binding protein HuD and transcription factor SATB1 promotes neurogenesis. *Proc. Natl. Acad. Sci. U.S.A.* **112,** E4995–5004
39. Lee, E. K., Kim, W., Tominaga, K., Martindale, J. L., Yang, X., Subaran, S. S., Carlson, O. D., Mercken, E. M., Kulkarni, R. N., Akamatsu, W., Okano, H., Perrone-Bizzozero, N. I., de Cabo, R., Egan, J. M., and Gorospe, M. (2012) RNA-binding protein HuD controls insulin translation. *Mol. Cell* **45,** 826–835
40. Kim, C., Kim, W., Lee, H., Ji, E., Choe, Y. J., Martindale, J. L., Akamatsu, W., Okano, H., Kim, H. S., Nam, S. W., Gorospe, M., and Lee, E. K. (2014) The RNA-binding protein HuD regulates autophagosome formation in pancreatic beta cells by promoting autophagy-related gene 5 expression. *J. Biol. Chem.* **289,** 112–121
41. Kim, C., Lee, H., Kang, H., Shin, J. J., Tak, H., Kim, W., Gorospe, M., and Lee, E. K. (2016) RNA-binding protein HuD reduces triglyceride production in pancreatic beta cells by enhancing the expression of insulin-induced gene 1. *Biochim. Biophys. Acta* **1859,** 675–685
42. Eizirik, D. L., Colli, M. L., and Ortis, F. (2009) The role of inflammation in insulitis and beta-cell loss in type 1 diabetes. *Nat. Rev. Endocrinol.* **5,** 219–226
43. Eizirik, D. L., Miani, M., and Cardozo, A. K. (2013) Signalling danger: endoplasmic reticulum stress and the unfolded protein response in pancreatic islet inflammation. *Diabetologia* **56,** 234–241
44. Brozzi, F., and Eizirik, D. L. (2016) ER stress and the decline and fall of pancreatic beta cells in type 1 diabetes. *Ups. J. Med. Sci.* **121,** 133–139
45. Jensen, K. B., Dredge, B. K., Stefani, G., Zhong, R., Buckanovich, R. J., Okano, H. J., Yang, Y. Y., and Darnell, R. B. (2000) Nova-1 regulates neuron-specific alternative splicing and is essential for neuronal viability. *Neuron* **25,** 359–371
46. Ule, J., Ule, A., Spencer, J., Williams, A., Hu, J. S., Cline, M., Wang, H., Clark, T., Fraser, C., Ruggiu, M., Zeeberg, B. R., Kane, D., Weinstein, J. N., Blume, J., and Darnell, R. B. (2005) Nova regulates brain-specific splicing to shape the synapse. *Nat. Genet.* **37,** 844–852
47. Zhang, C., Frias, M. A., Mele, A., Ruggiu, M., Eom, T., Marney, C. B., Wang, H., Licatalosi, D. D., Fak, J. J., and Darnell, R. B. (2010) Integrative

modeling defines the Nova splicing-regulatory network and its combinatorial controls. *Science* **329,** 439–443
48. Leggere, J. C., Saito, Y., Darnell, R. B., Tessier-Lavigne, M., Junge, H. J., and Chen, Z. (2016) NOVA regulate alternative splicing during neuronal migration and axon guidance in the spinal cord. *Elife* **5,** e14264
49. Lovci, M. T., Ghanem, D., Marr, H., Arnold, J., Gee, S., Parra, M., Liang, T. Y., Stark, T. J., Gehman, L. T., Hoon, S., Massirer, K. B., Pratt, G. A., Black, D. L., Gray, J. W., Conboy, J. G., and Yeo, G. W. (2013) Rbfox proteins regulate alternative mRNA splicing through evolutionarily conserved RNA bridges. *Nat. Struct. Mol. Biol.* **20,** 1434–1442
50. Saito, Y., Miranda-Rottmann, S., Ruggiu, M., Park, C. Y., Fak, J. J., Zhong, R., Duncan, J. S., Fabella, B. A., Junge, H. J., Chen, Z., Araya, R., Fritzsch, B., Hudspeth, A. J., and Darnell, R. B. (2016) NOVA2-mediated RNA regulation is required for axonal pathfinding during development. *Elife* **5,** e14371
51. Fogel, B. L., Wexler, E., Wahnich, A., Friedrich, T., Vijayendran, C., Gao, F., Parikshak, N., Konopka, G., and Geschwind, D. H. (2012) RBFOX1 regulates both splicing and transcriptional networks in human neuronal development. *Hum. Mol. Genet.* **21,** 4171–4186
52. Gehman, L. T., Meera, P., Stoilov, P., Shiue, L., O'Brien, J. E., Meisler, M. H., Ares MJr, Otis, T. S., and Black, D. L. (2012) The splicing regulator Rbfox2 is required for both cerebellar development and mature motor function. *Genes Dev.* **26,** 445–460
53. Bhalla, K., Phillips, H. A., Crawford, J., McKenzie, O. L., Mulley, J. C., Eyre, H., Gardner, A. E., Kremmidiotis, G., and Callen, D. F. (2004) The de novo chromosome 16 translocations of two patients with abnormal phenotypes (mental retardation and epilepsy) disrupt the A2BP1 gene. *J. Hum. Genet.* **49,** 308–311
54. Xu, B., Roos, J. L., Levy, S., van Rensburg, E. J., Gogos, J. A., and Karayiorgou, M. (2008) Strong association of *de novo* copy number mutations with sporadic schizophrenia. *Nat. Genet.* **40,** 880–885
55. Martin, C. L., Duvall, J. A., Ilkin, Y., Simon, J. S., Arreaza, M. G., Wilkes, K., Alvarez-Retuerto, A., Whichello, A., Powell, C. M., Rao, K., Cook, E., and Geschwind, D. H. (2007) Cytogenetic and molecular characterization of A2BP1/FOX1 as a candidate gene for autism. *Am. J. Med. Genet. B Neuropsychiatr. Genet.* **144,** 869–876
56. Sebat, J., Lakshmi, B., Malhotra, D., Troge, J., Lese-Martin, C., Walsh, T., Yamrom, B., Yoon, S., Krasnitz, A., Kendall, J., Leotta, A., Pai, D., Zhang, R., Lee, Y. H., Hicks, J., *et al.* (2007) Strong association of *de novo* copy number mutations with autism. *Science* **316,** 445–449
57. Pedrotti, S., Giudice, J., Dagnino-Acosta, A., Knoblauch, M., Singh, R. K., Hanna, A., Mo, Q., Hicks, J., Hamilton, S., and Cooper, T. A. (2015) The RNA-binding protein Rbfox1 regulates splicing required for skeletal muscle structure and function. *Hum. Mol. Genet.* **24,** 2360–2374
58. Eliasson, L., Abdulkader, F., Braun, M., Galvanovskis, J., Hoppa, M. B., and Rorsman, P. (2008) Novel aspects of the molecular mechanisms controlling insulin secretion. *J. Physiol.* **586,** 3313–3324
59. Henquin, J. C. (2009) Regulation of insulin secretion: a matter of phase control and amplitude modulation. *Diabetologia* **52,** 739–751
60. Kalwat, M. A., and Thurmond, D. C. (2013) Signaling mechanisms of glucose-induced F-actin remodeling in pancreatic islet beta cells. *Exp. Mol. Med.* **45,** e37
61. Gilon, P., Chae, H. Y., Rutter, G. A., and Ravier, M. A. (2014) Calcium signaling in pancreatic beta-cells in health and in Type 2 diabetes. *Cell Calcium* **56,** 340–361
62. Gallagher, T. L., Arribere, J. A., Geurts, P. A., Exner, C. R., McDonald, K. L., Dill, K. K., Marr, H. L., Adkar, S. S., Garnett, A. T., Amacher, S. L., and Conboy, J. G. (2011) Rbfox-regulated alternative splicing is critical for zebrafish cardiac and skeletal muscle functions. *Dev. Biol.* **359,** 251–261
63. Giulietti, M., Piva, F., D'Antonio, M., D'Onorio De Meo, P., Paoletti, D., Castrignanò, T., D'Erchia, A. M., Picardi, E., Zambelli, F., Principato, G., Pavesi, G., and Pesole, G. (2013) SpliceAid-F: a database of human splicing factors and their RNA-binding sites. *Nucleic Acids Res.* **41,** D125–D131
64. Reich, M., Liefeld, T., Gould, J., Lerner, J., Tamayo, P., and Mesirov, J. P. (2006) Gene Pattern 2.0. *Nat. Genet.* **38,** 500–501
65. Ortis, F., Cardozo, A. K., Crispim, D., Störling, J., Mandrup-Poulsen, T., and Eizirik, D. L. (2006) Cytokine-induced proapoptotic gene expression in insulin-producing cells is related to rapid, sustained, and nonoscillatory nuclear factor-κB activation. *Mol. Endocrinol.* **20,** 1867–1879
66. Marroqui, L., Masini, M., Merino, B., Grieco, F. A., Millard, I., Dubois, C., Quesada, I., Marchetti, P., Cnop, M., and Eizirik, D. L. (2015) Pancreatic alpha cells are resistant to metabolic stress-induced apoptosis in type 2 diabetes. *EBioMedicine* **2,** 378–385
67. Ravassard, P., Hazhouz, Y., Pechberty, S., Bricout-Neveu, E., Armanet, M., Czernichow, P., and Scharfmann, R. (2011) A genetically engineered human pancreatic beta cell line exhibiting glucose-inducible insulin secretion. *J. Clin. Invest.* **121,** 3589–3597
68. Brozzi, F., Nardelli, T. R., Lopes, M., Millard, I., Barthson, J., Igoillo-Esteve, M., Grieco, F. A., Villate, O., Oliveira, J. M., Casimir, M., Bugliani, M., Engin, F., Hotamisligil, G. S., Marchetti, P., and Eizirik, D. L. (2015) Cytokines induce endoplasmic reticulum stress in human, rat and mouse beta cells via different mechanisms. *Diabetologia* **58,** 2307–2316
69. Lupi, R., Dotta, F., Marselli, L., Del Guerra, S., Masini, M., Santangelo, C., Patané, G., Boggi, U., Piro, S., Anello, M., Bergamini, E., Mosca, F., Di Mario, U., Del Prato, S., and Marchetti, P. (2002) Prolonged exposure to free fatty acids has cytostatic and pro-apoptotic effects on human pancreatic islets: evidence that beta-cell death is caspase mediated, partially dependent on ceramide pathway, and Bcl-2 regulated. *Diabetes* **51,** 1437–1442
70. Moore, F., Colli, M. L., Cnop, M., Esteve, M. I., Cardozo, A. K., Cunha, D. A., Bugliani, M., Marchetti, P., and Eizirik, D. L. (2009) PTPN2, a candidate gene for type 1 diabetes, modulates interferon-γ-induced pancreatic beta-cell apoptosis. *Diabetes* **58,** 1283–1291
71. Eizirik, D. L., Pipeleers, D. G., Ling, Z., Welsh, N., Hellerström, C., and Andersson, A. (1994) Major species differences between humans and rodents in the susceptibility to pancreatic beta-cell injury. *Proc. Natl. Acad. Sci. U.S.A.* **91,** 9253–9256
72. Heimberg, H., Heremans, Y., Jobin, C., Leemans, R., Cardozo, A. K., Darville, M., and Eizirik, D. L. (2001) Inhibition of cytokine-induced NF-κB activation by adenovirus-mediated expression of an NF-κB super-repressor prevents beta-cell apoptosis. *Diabetes* **50,** 2219–2224
73. Moore, F., Cunha, D. A., Mulder, H., and Eizirik, D. L. (2012) Use of RNA interference to investigate cytokine signal transduction in pancreatic beta cells. *Methods Mol. Biol.* **820,** 179–194
74. Cardozo, A. K., Ortis, F., Storling, J., Feng, Y. M., Rasschaert, J., Tonnesen, M., Van Eylen, F., Mandrup-Poulsen, T., Herchuelz, A., and Eizirik, D. L. (2005) Cytokines downregulate the sarcoendoplasmic reticulum pump Ca^{2+} ATPase 2b and deplete endoplasmic reticulum Ca^{2+}, leading to induction of endoplasmic reticulum stress in pancreatic beta-cells. *Diabetes* **54,** 452–461
75. Rasschaert, J., Ladrière, L., Urbain, M., Dogusan, Z., Katabua, B., Sato, S., Akira, S., Gysemans, C., Mathieu, C., and Eizirik, D. L. (2005) Toll-like receptor 3 and STAT-1 contribute to double-stranded RNA+ interferon-γ-induced apoptosis in primary pancreatic beta-cells. *J. Biol. Chem.* **280,** 33984–33991
76. Eizirik, D. L., Sandler, S., Sener, A., and Malaisse, W. J. (1988) Defective catabolism of D-glucose and L-glutamine in mouse pancreatic islets maintained in culture after streptozotocin exposure. *Endocrinology* **123,** 1001–1007
77. Andersson, L. E., Valtat, B., Bagge, A., Sharoyko, V. V., Nicholls, D. G., Ravassard, P., Scharfmann, R., Spégel, P., and Mulder, H. (2015) Characterization of stimulus-secretion coupling in the human pancreatic EndoC-βH1 beta cell line. *PLoS ONE* **10,** e0120879
78. Vikman, J., Ma, X., Hockerman, G. H., Rorsman, P., and Eliasson, L. (2006) Antibody inhibition of synaptosomal protein of 25 kDa (SNAP-25) and syntaxin 1 reduces rapid exocytosis in insulin-secreting cells. *J. Mol. Endocrinol.* **36,** 503–515
79. Cnop, M., Ladriere, L., Hekerman, P., Ortis, F., Cardozo, A. K., Dogusan, Z., Flamez, D., Boyce, M., Yuan, J., and Eizirik, D. L. (2007) Selective inhibition of eukaryotic translation initiation factor 2α dephosphorylation potentiates fatty acid-induced endoplasmic reticulum stress and causes pancreatic beta-cell dysfunction and apoptosis. *J. Biol. Chem.* **282,** 3989–3997
80. Wallenstein, S., Zucker, C. L., and Fleiss, J. L. (1980) Some statistical methods useful in circulation research. *Circ. Res.* **47,** 1–9

Neuron-enriched RNA-binding Proteins Regulate Pancreatic Beta Cell Function and Survival

Jonàs Juan-Mateu, Tatiana H. Rech, Olatz Villate, Esther Lizarraga-Mollinedo, Anna Wendt, Jean-Valery Turatsinze, Letícia A. Brondani, Tarlliza R. Nardelli, Tatiane C. Nogueira, Jonathan L. S. Esguerra, Maria Inês Alvelos, Piero Marchetti, Lena Eliasson and Décio L. Eizirik

J. Biol. Chem. 2017, 292:3466-3480.
doi: 10.1074/jbc.M116.748335 originally published online January 11, 2017
